ADSORPTION ISOTHERMS FOR SYSTEMS WITH ADSORPTION COMPRESSION

By:

Shao-Hsuan Lin

A thesis submitted to Johns Hopkins University in conformity with the requirements for the degree of Master of Science Engineering.

Baltimore, Maryland
May, 2018

Abstract

While there have been a large number of papers that have discussed the phenomena of adsorption compression, there is not yet an analytic model which can predict the adsorption isotherm for a system that exhibits adsorption compression. This thesis presents such a model. To have adsorption compression, the adsorbate molecules must be "soft" and here Lennard-Jones molecules are used to predict adsorption compression. If we define the adsorption to be unity when the adsorbate-adsorbate distances are at the minimum of their intermolecular potential energy function, the adsorption can exceed unity when the attractive force caused by the surface is stronger than repulsive forces caused by other adsorbate molecules on the surface. This new model allows prediction of the density of adsorbate molecules on a solid surface as a function of the energies of adsorbate-adsorbent and adsorbate-adsorbate interactions and the density or chemical potential of the adsorptive in the bulk. For a system of argon molecules adsorbed on a solid surface with adsorbate-adsorbent energy of -5.0kT, and adsorbate-adsorbate energy of -0.5kT, the adsorption can be as high as 1.4.

Adsorption compression can lead to several interesting phenomena including Graphene-like and checkerboard-like patterns on the surface.

Thesis Committee:

Marc D. Donohue, Professor of Chemical Engineering

Gregory L. Aranovich, Research Professor of Chemical Engineering

Table of Contents

Acknowledgements

I would like to give my most sincere appreciation to Professor Marc D. Donohue, who had been leading me through the difficulties for the past two years with my graduate research. Under the guidance of the best supervisor in the Chemical and Biomolecular Engineering Department of Johns Hopkins University, I was able to develop an analytical model for predicting adsorption isotherms with adsorption compression. Another person I would like to thank from the bottom of my heart is Dr. Gregory L. Aranovich for not only giving me a big hand with my research, but also instructing me on knowledge about adsorption compression.

Also, I would like to thank my parents for the full support for me to study in such a decent school as Johns Hopkins University. Since I was a child, they had been telling me that the process is more important than the result. Although the consequence is important, what have I learned from the process matters much more.

List of Figures

neighbors (1), and 2nd nearest neighbors (2).

Figure 16. Dependence of ρ_1 (I), ρ_2 (II), ρ_1' (III), and ρ_1'' (IV) on ρ_b at various σ/d: (a)1.01, (b)1.02, (c)1.03, (d)1.04, (e)1.05, (f)1.06, (g)1.07, (h)1.08, (i)1.09, and (j)1.10 and $\varphi_s/kT = -5.0$.

Figure 17. Dependence of ρ_1 (I), ρ_2 (II), ρ_1' (III), and ρ_1'' (IV) and right-hand-side of equation (26) on ρ_b at various σ/d: (a)1.052, (b)1.053, (c)1.054, (d)1.055.

Figure 18. Dependence of ρ_1 (I), ρ_2 (II), ρ_1' (III), and ρ_1'' (IV) on ρ_b with an auxiliary line ($x - y = 0$) at $(\sigma/d) = 1.053$.

Figure 19. Dependence of ρ_1 (I), ρ_2 (II), ρ_1' (III), and ρ_1'' (IV) on the bulk density for various σ/d: (a)1.02, (b)1.04, (c)1.06, (d)1.08, and (e)1.10.

Figure 20. Dependence of ρ_1 (I), ρ_2 (II), ρ_1' (III), and ρ_1'' (IV) on the bulk density for $(\varphi_s/kT) = -3.0$ at various σ/d: (a)1.01, (b)1.02, (c)1.03, (d)1.04, (e)1.05, (f)1.06, (g)1.07, (h)1.08, (i)1.09, and (j)1.10.

Figure 21. Dependence of ρ_1 (I), ρ_2 (II), ρ_1' (III), and ρ_1'' (IV) on the bulk density for $(\varphi_s/kT) = -10.0$ at various σ/d: (a)1.01, (b)1.02, (c)1.03, (d)1.04, (e)1.05, (f)1.06, (g)1.07, (h)1.08, (i)1.09, and (j)1.10.

Figure 22. Dependence of ρ_1 (a, c, e) (solid lines) and ρ_2 (b, d, f) (dashed lines) on the bulk density for $\sigma/d =$ 1.05 (I) and 1.06 (II), and different φ_s/kT: -3.0 (a, b), -5.0 (c, d), and -10.0 (e, f).

Figure 23. The average density as a function of the bulk density for φ_s/kT: -3.0 (I), -5.0 (II), and -10.0 (III) at various σ/d: (a) $2^{-1/6}$, (b) 1.00, (c) 1.05, (d) 1.06, (e) 1.07, (f) 1.08, (g) 1.09, and (h) 1.10.

1. Introduction

Sorption: Ad- vs. Ab-

Sorption is a process where molecules of one substance are attached to molecules of another substance. It can involve physical or chemical interactions. There are three main categories of sorption: adsorption, absorption, and ion exchange[1]. The difference between adsorption and absorption is demonstrated in Figure 1. Adsorption happens when there is adherence of a molecule to a surface, while absorption happens when molecules of one species are dissolved into another species. IUPAC defines adsorption as "An increase in the concentration of a dissolved substance at the interface of a condensed and a liquid phase due to the operation of surface forces. Adsorption also can occur at the interface of a condensed and a gaseous phase."[2]

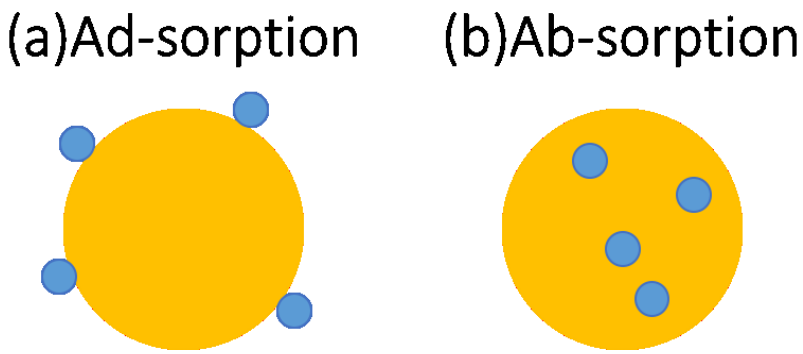

Figure 1. Schematic illustration to (a) adsorption, and (b) absorption, where molecules (a) adhere to the surface, and (b) are drawn into solution.

Theories of Adsorption

Physical adsorption of gas on solid or liquid surface depends on temperature, pressure, density, and the energies of adsorbate-adsorbent and adsorbate-adsorbate interactions. Among all classical theories, Langmuir's model is the best known and most widely used adsorption isotherm[4]. It assumes monolayer adsorption and neglects lateral (adsorbate-adsorbate) interactions. From these assumptions, we can derive the Langmuir isotherm for molecule A:

$$\theta_A = \frac{K_{eq}^A p_A}{1+K_{eq}^A p_A} \quad (1)$$

where θ_A is the fraction occupancy by the adsorbate A, K_{eq}^A is the equilibrium constant, p_A is the partial pressure of the molecule being adsorbed, A.

To make Langmuir's theory closer to realistic adsorption mechanisms, more sophisticated models have been proposed. In particular, Frumkin[5] and Fowler and Guggenheim[6], developed a model which takes into account lateral (adsorbate-adsorbate) interactions. This model can predict two-dimensional phase transitions in the adsorbed layer; however, perpendicular (interlayer) interactions are not taken into account and multilayer adsorption is not predicted. Brunauer, Emmett, and Teller (BET)[7] derived multilayer adsorption isotherm by considering interlayer interactions,

but neglecting lateral interactions (Figure 2). Thus, the three-dimensional problem is turned into one-dimensional, lacking of consideration of two-dimensional phase transition. The BET equation for multilayer adsorption isotherm is the following:

$$a = \frac{a_m c x_A}{(1-x_A)[1-x_A(1-c)]} \tag{2}$$

where a is the adsorbed amount, a_m is the monolayer capacity, c is the BET constant, and x_A is the ratio of equilibrium pressure divided by saturation pressure (p/p_0) of adsorbate.

In terms of adsorption mechanisms, the BET model is oversimplified. However, it captures general features of adsorption isotherms and it is widely used in surface science.

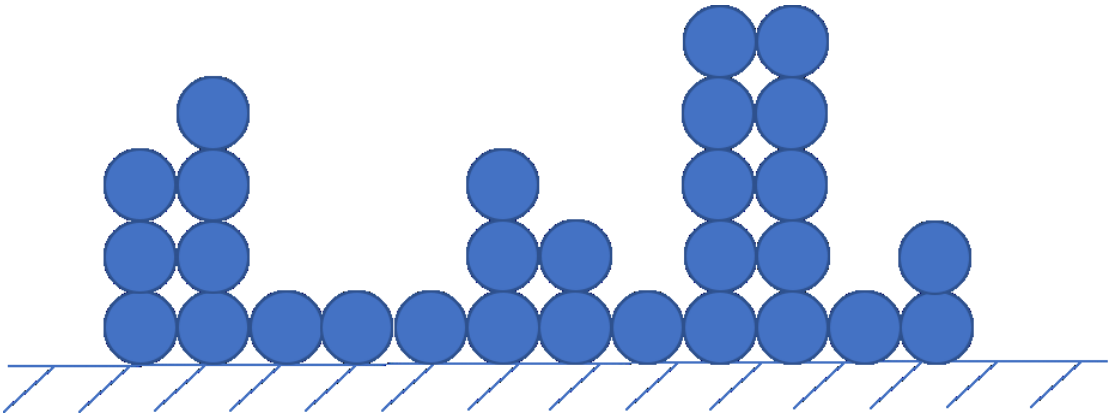

Figure 2. The BET model for multilayer adsorption on surfaces

Other theories have been developed to incorporate other factors, including models with long-range molecule-surface interactions[8], potential theory of adsorption[9,10], molecular simulations and statistical mechanical calculations[11], real structure oriented potential theory of adsorption[12], and models taking into account structure of micro-pores[13].

One of the most important ideas for density gradients at vapor-liquid interfaces was proposed by Ono and Kondo[14], which was later used to develop lattice density functional theory (LDFT) to study fluids in a confined environment[15-18]. LDFT of adsorption is widely used for modeling adsorption isotherms and studying adsorption mechanisms, including the recently discovered phenomenon of adsorption compression[19-27].

Figure 3 illustrates adsorption compression in the framework of a two-site model, where the distance between two sites dramatically affects adsorption isotherm. Adsorption compression appears when affinity to the adsorbent is strong enough that lateral repulsions can be balanced by molecule-surface interactions[28].

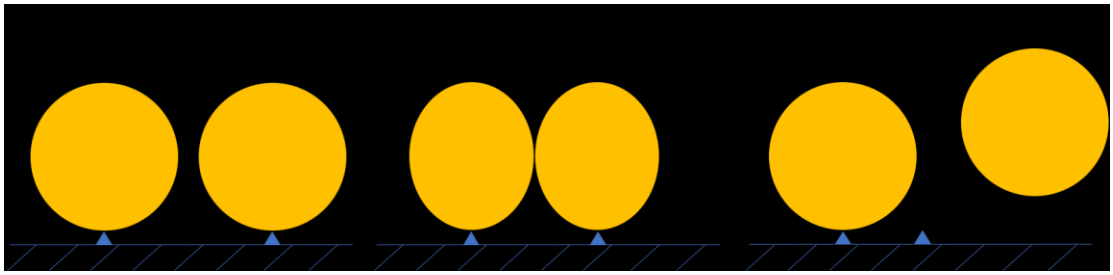

Figure 3. The distance between two active sites is (a) large, so that molecules can adsorb on both of these sites independently; (b) intermediate, so that molecules can sit on these sites being compressed; and (c) small, so that a molecule on one of the sites blocks the other site.

Lennard-Jones Potential

The Lennard-Jones potential, also known as 12-6 potential, was first introduced in 1924, by John Lennard-Jones[28]. It is a mathematically simple approximation for interatomic interactions between two neutral atoms or molecules. The most common Lennard-Jones potential can be written as:

$$\varphi(\sigma) = 4\epsilon_o[\left(\frac{d}{\sigma}\right)^{12} - \left(\frac{d}{\sigma}\right)^{6}] \quad (3)$$

where $\varphi(\sigma)$ is the Lennard-Jones potential function, ϵ_o is the depth of the potential well, d is the distance at which the energy of interaction between two molecules is zero, σ is the distance between the two molecules. In equation (3), the 12^{th} power term accounts for repulsions, and the 6^{th} power term accounts for attractions.

Figure 4 illustrates Lennard-Jones potential function, $\varphi(\sigma)$, in normalized coordinates: y-axis shows $\varphi(\sigma)/\epsilon_o$ and x-axis shows d/σ where d is the distance between adsorbed molecules, and σ is the distance between adsorbed molecules when the energy between the molecules is zero. I.E., σ is the diameter of the adsorbed molecules. Thus, when $d/\sigma < 1$, the distance between adsorption sites is less than the distance between two molecules at zero energy, and the Lennard-Jones potential is repulsive, as shown on left-hand-side of point (a) in Figure 4. When $d/\sigma = 1$, there are no forces between the two molecules, as shown of point (a) in Figure 4. The Lennard-Jones potential reaches its minimum at $d = 2^{1/6}\sigma$, as shown of point (b) in Figure 4. Typically, the average intermolecular distance in a normal liquid is somewhat greater than that of the minimum in the potential function.

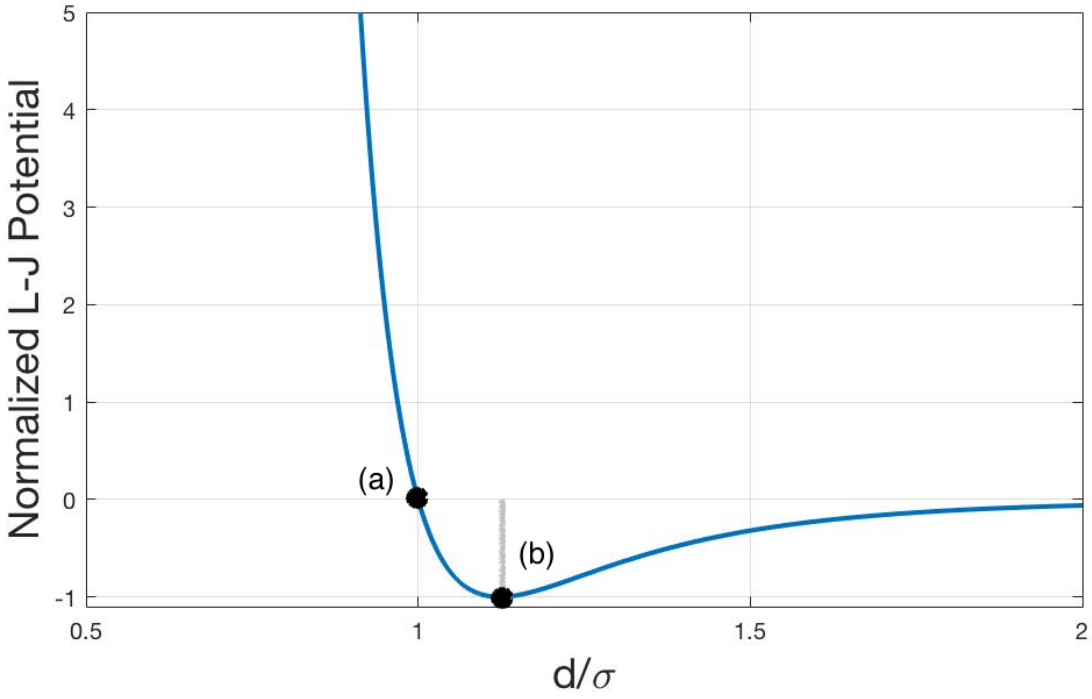

Figure 4. Normalized Lennard-Jones potential function

Adsorption Compression

Describing realistic adsorption behavior is the primary goal of adsorption theories. A new phenomenon discovered by the analysis of adsorption data is adsorption compression. Figure 5 illustrates thermodynamic reasons for adsorption compression in a monolayer. The adsorbed amount goes up until the point where lateral repulsions are balanced by adsorbate-adsorbent interaction. As more and more adsorbate molecules are pulled onto the surface, the surface will become more and more crowded, which leads to shorter distance between adsorbate molecules.

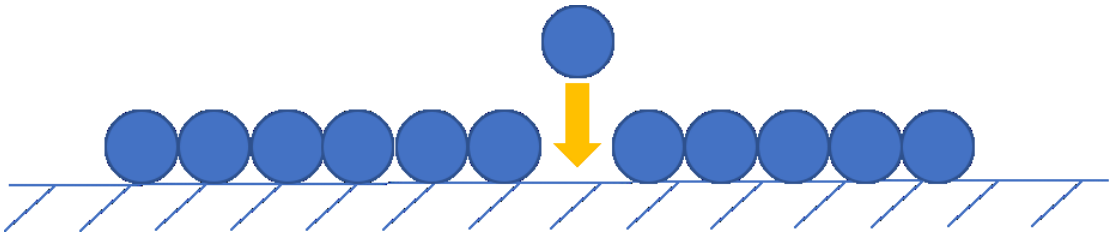

Figure 5. Thermodynamic reasons for surface compression

Adsorption compression has been observed in systems with both chemisorption and physisorption. Adsorption compression has been seen for , oxygen (O_2) on nickel (Ni) surface (Al-Sarraf and King[29]), for carbon monoxide (CO) on Rhodium (Rh{100}) surface (Kose et al.[30]), for CO on platinum (Pt{110}) surface and hydrogen (H_2) on zinc oxide (ZnO) surface (Molinari and Tomellini[31]), for neon (Ne), argon (Ar), nitrogen (N_2), and xenon (Xe) on graphite surface (Eber[32]), and for magnesium chloride ($MgCl_2$) on several metal crystal surfaces such as palladium (Pd{111}), Pt(111), and Rh(111) (Fairbrother et al.[33]). Adsorption compression was observed and analyzed in simulations and in theoretical considerations[34, 35] for different systems, including adsorptions of Ar on Pt(111) and Ne and Xe on graphite (by Charniak et al.[34]).

2. Adsorption Isotherms for Systems with Adsorption Compression

The simplest case of adsorption compression is for adsorption of two molecules on two active sites. This is important in applications for catalysis, because two molecules sitting on two sites with adsorption compression will have a lower activation energy than when there is no adsorption compression.

For a monolayer, adsorption compression can be caused by confinement imposed by capacity of the monolayer. For the full monolayer, adsorbate molecules repel each other and the distance between neighbors is less than that in a normal liquid.

The adsorption "thermaldynamic" capacity, a_m, is the adsorbed amount when adsorbate-adsorbent attractive force is balanced by repulsive force in lateral interactions. In the previous models, a_m is often treated as a constant which means that it does not depend on energies of adsorbate-adsorbate and adsorbate-adsorbent interactions. As the adsorbed amount approaches a_m, the differential heat of adsorption must disappear due to surface compression.

Ono-Kondo Equation Approach

In this analysis, we assume that:

- the surface is homogeneous;

- adsorbate molecules are in a monolayer on the surface of the adsorbent;

- there is some average energy of interaction, φ_s, between each adsorbate molecule and the surface;

- the energy of interaction between adsorbate molecules, φ, can be described by the Lennard-Jones potential function[28] [equation (3)].

Consider taking an adsorbate molecule form an adsorption site on the surface and putting it into an empty space between molecules in the bulk:

$$M_s + V_b = V_s + M_b \tag{4}$$

where M_s is the adsorbate molecule on the surface, M_b is the adsorbate molecule in the bulk, V_s is the vacancy on the surface, V_b is the vacancy in the bulk. When the exchange of molecule occurs at equilibrium, the free energy, ΔG, equals to zero,

$$\Delta G = \Delta H - T\Delta S = 0 \tag{5}$$

Here ΔH is the enthalpy change, T is the absolute temperature, and ΔS is the entropy change. In the framework of mean-field approximation, the terms ΔH and ΔS can be represented by the following equations:

$$\begin{cases} \Delta H = \frac{\varphi_s}{kT} + Z\frac{\varphi}{kT}X_a - Z_b\frac{\varphi_b}{kT}X_b \\ \Delta S = k\ln\frac{(a/a_m)(1-X_b)}{(1-a/a_m)X_b} \end{cases} \tag{6}$$

where a is the density of the adsorbed layer[36], a_m is the monolayer capacity, $X_a = a/a_m$ and X_b are the densities of adsorbate on the surface and in the bulk. Since $\Delta H = \Delta U + P\Delta V$ and there is no volume change, $\Delta H = \Delta U$, where ΔU is the internal energy change. Here Z and Z_b are coordination numbers on the surface and in the bulk. Then equation of equilibrium can be written in the following form:

$$\ln\frac{X_a}{1-X_a} + \frac{\varphi_s}{kT} + Z\frac{\varphi}{kT}X_a = \ln\frac{X_b}{1-X_b} + Z_b\frac{\varphi_b}{kT}X_b \tag{7}$$

After algebraic manipulations, equation (7) can be presented as follows:

$$\frac{X_a}{1-X_a}e^{\frac{\varphi_s}{kT}+Z\frac{\varphi}{kT}X_a} = \frac{X_b}{1-X_b}e^{Z_b\frac{\varphi_b}{kT}X_b} \tag{8}$$

If the energy of adsorptive-bulk interaction is negligible compared to the energy of a molecule in adsorbed layer then equation (8) gives:

$$X_a = \frac{X_b}{X_b+(1-X_b)e^{\frac{\varphi_s}{kT}+Z\frac{\varphi}{kT}X_a}} \tag{9}$$

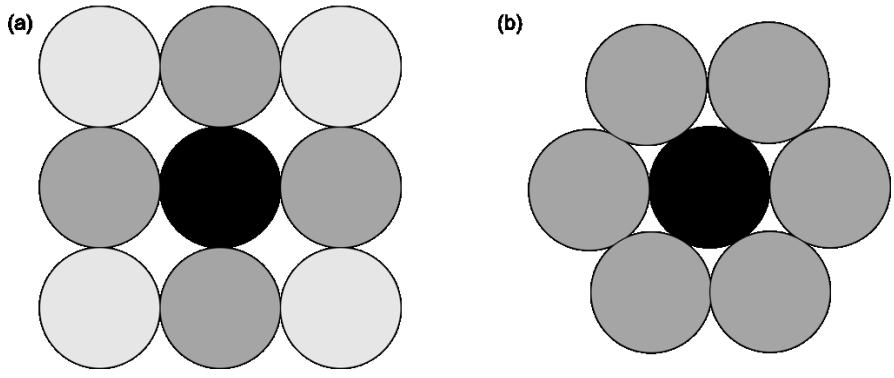

Figure 6. Neighboring molecules (colored gray) for a randomly chosen central molecule (colored black) for (a) square system, and (b) hexagonal system.

New Model of Analytical Method

Equation (8) can be written as

$$\frac{\mu}{kT} = \ln\frac{X_b}{1-X_b} = \frac{\varphi_s}{kT} + Z\frac{\varphi}{kT}X_a + \ln\frac{X_a}{1-X_a} \tag{10}$$

where μ/kT is the change of the chemical potential due to exchange. Note that $\ln[X_b/(1-X_b)]$ is the change of the chemical potential in the bulk and $\varphi_s/kT + Z(\varphi/kT)X_a + \ln[X_a/(1-X_a)]$ is the change of the chemical potential in adsorbed phase. Defining $X_a = N_a/N_s$, where N_a is the number of molecules adsorbed, N_s is the number of adsorption sites. Let the interaction distance between two adsorbates, σ, equal to $\sqrt{s/N_s}$, where s is the area of the surface. Using the Lennard-Jones potential equation (10) gives:

$$\ln\frac{X_b}{1-X_b} = \frac{\varphi_s}{kT} + 4Z\frac{\epsilon_o}{kT}N_a\left(\frac{\sigma^6 N_s^2}{s^3} - \frac{\sigma^{12}N_s^5}{s^6}\right) + \ln\frac{N_a}{N_s - N_a} \tag{11}$$

Equation (11) has two unknowns, N_a and N_s. To determine them, we need a second equation to allow us to choose the right number of sites for each number of adsorbed molecules. To do that, consider the chemical potential as a function of N_s at constant N_a. With these constraints, the chemical potential can be defined as free energy divided by number of molecules, $\mu = (U - TS)/N_a$ [see equation (7.11) in page 28 of Reference 37]. Therefore, at constant number of molecules, $U - TS = \mu N_a$

and minimum of free energy, $U - TS$, is equivalent to the minimum of chemical potential. Therefore, in this case:

$$\left.\frac{\partial(\mu/kT)}{\partial N_s}\right|_{N_a} = 0 \tag{12}$$

$$4Z\frac{\epsilon_o}{kT}N_a\frac{\sigma^6 N_s}{s^3}\left(2 - \frac{5\sigma^6 N_s^3}{s^3}\right)(N_s - N_a) = 1 \tag{13}$$

Simplification of variables: $n_a = N_a/s$, $n_s = N_s/s$. Then equations (12) and (13) become:

$$\ln\frac{X_b}{1-X_b} = \frac{\varphi_s}{kT} + 4z\frac{\epsilon_o}{kT}\sigma^6 n_s^2(1 - \sigma^6 n_s^3)n_a + \ln\frac{n_a}{n_s - n_a} \tag{14}$$

$$4z\frac{\epsilon_o}{kT}\sigma^6 n_s(2 - 5\sigma^6 n_s^3)(n_s - n_a)n_a = 1 \tag{15}$$

Equations (14) and (15) determine the isotherm which can be given by equation (15) as X_b versus n_a for n_s determined by equation (14). Using the notation:

$$f(n_s) = 4z\frac{\epsilon_o}{kT}\sigma^6 n_s(2 - 5\sigma^6 n_s^3) \tag{16}$$

equation (15) can be rewritten in the following form:

$${n_a}^2 - n_s \times n_a + \frac{1}{f} = 0 \tag{17}$$

The solution of equation (17) is:

$$n_{a_{1,2}} = \frac{n_s}{2}\left[1 \pm \sqrt{1 - \frac{1}{Z\frac{\epsilon_o}{kT}\sigma^6 n_s^3(2 - 5\sigma^6 n_s^3)}}\right] \tag{18}$$

Let $q = \sigma^6 n_s^3$, and $X_a = n_a/n_s$, which gives instead of equations (14) and (18):

$$X_{a_{1,2}} = \frac{1}{2}\left[1 \pm \sqrt{1 - \frac{1}{Z\frac{\epsilon_o}{kT}q(2 - 5q)}}\right] \tag{19}$$

$$\ln\frac{X_b}{1-X_b} = \frac{\varphi_s}{kT} + 4Z\frac{\epsilon_o}{kT}q(1-q)X_a + \ln\frac{X_a}{1-X_a} \quad (20)$$

Equations (19) and (20) define X_a versus X_b in a parametric form where q is a parameter.

Results and Discussions

To demonstrate the adsorption isotherm for systems with adsorption compression, the analytical solution is compared with the Ono-Kondo model[14] and with the numerical solution[38]. In the analytical solution, we set $\sigma = 3.499$Å, $\epsilon_o/kT = 0.5$, $\varphi_s/kT = -5.0$, and $Z = 4$. In numerical solution, molecules are added to the surface one at a time until X_b is over 99%. Once a molecule is added onto the surface, two different conditions are calculated, one is for no site added, the other is one site added on the surface while there is a constraint that adsorption sites are not allowed to be added before 50% of the initial number of sites are occupied by adsorbate molecules. The average distance of adsorbate molecules is changed as the total number of adsorption sites is increased by one each time, which gives two different Lennard-Jones potentials [equation (3)] and leads to different number of X_b, the condition with lower X_b is selected for the numerical method.

Figure 7 illustrates the comparison of these three models. The Ono-Kondo model

has the largest X_a value while X_b approaches unity. The analytical solution and numerical solution agree with each other, but their predictions differ from prediction of the original Ono-Kondo model.

To analyze adsorption compression, replace X_a by X_a^*, which is related on initial number of adsorption sites rather than total number of sites, that is,

$$X_a^* = X_a \times \ (a_m/a_{mh}) \tag{21}$$

where a_{mh} is monolayer adsorption capacity for hard molecules. This parameter, a_m/a_{mh}, shows the difference in capacity between hard molecules and Lennard-Jones (soft) molecules, and it is always ≥ 1 since the soft molecules can pack closer to each other than hard molecules.

Figure 8 shows dependence of X_a^* on X_b. Models capturing adsorption compression [(equations (19) and (20)] and Ono-Kondo model without compression predict distinctly different isotherms. Due to adsorption compression, X_a^* exceeds unity while X_b is about 0.012. When $X_b = 0.99$, X_a^* becomes 1.40, indicates significant compression.

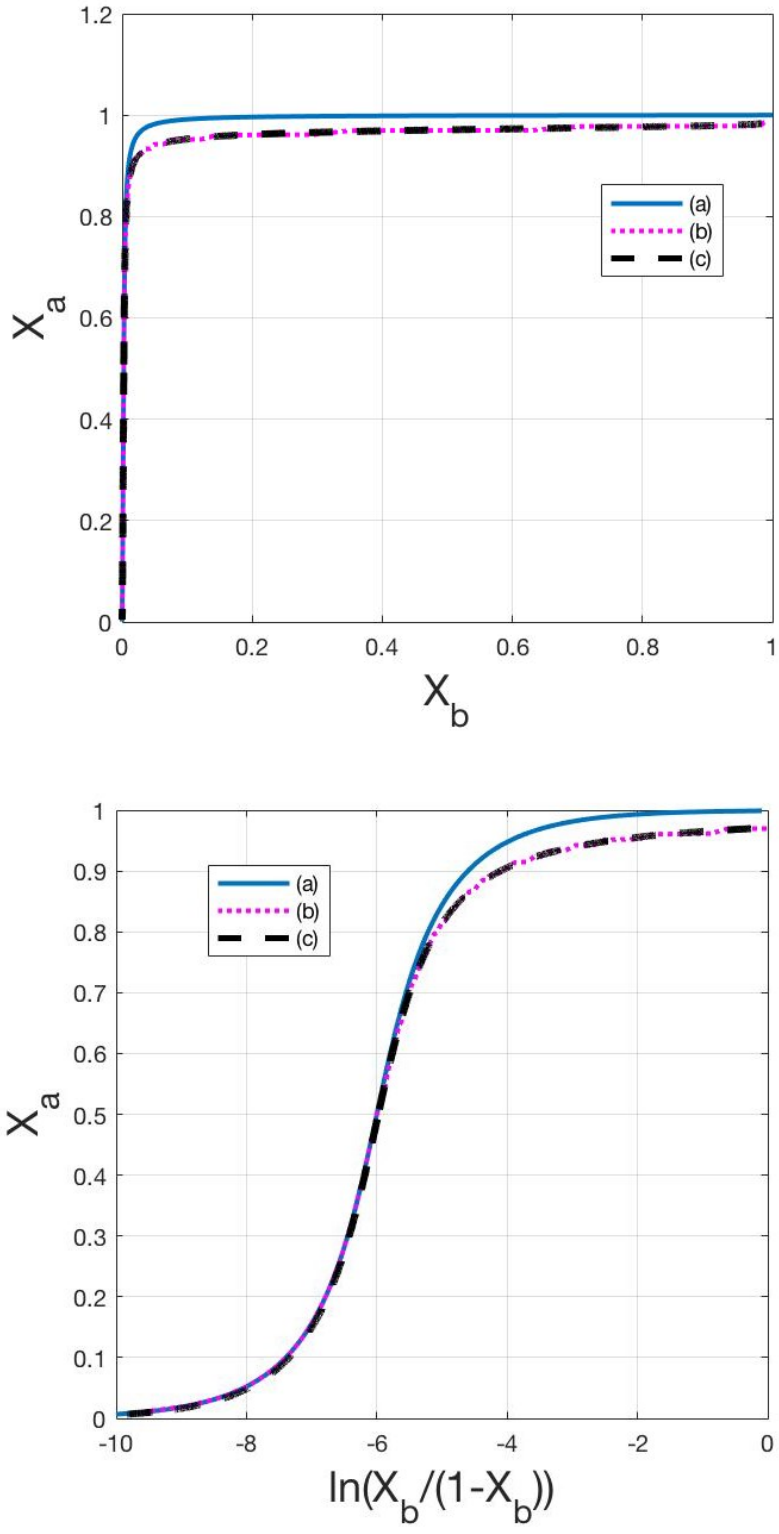

Figure 7. Adsorption isotherm predicted by different models: (a) Ono-Kondo, (b) numerical, and (c) analytical.

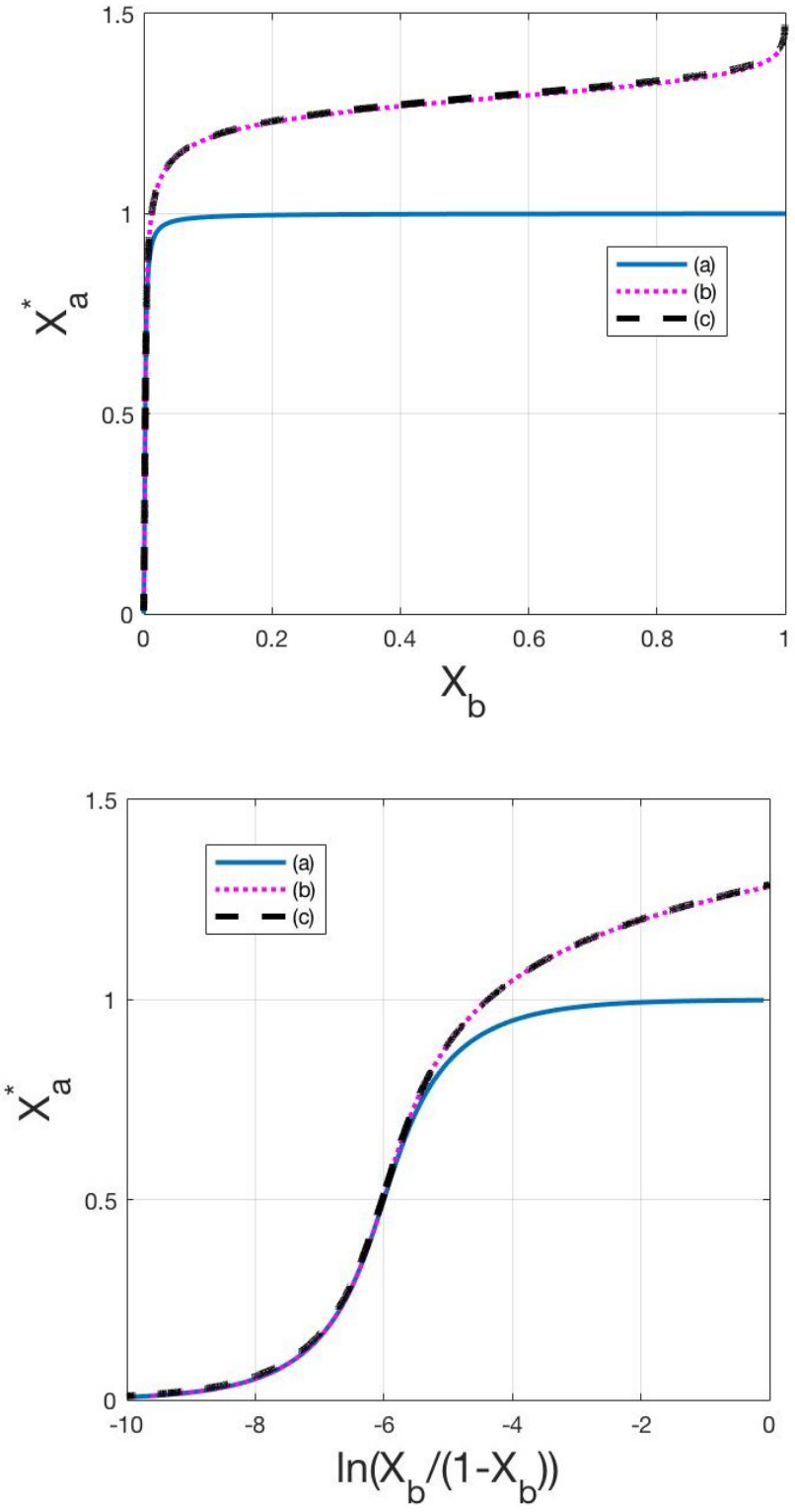

Figure 8. Adsorption compression isotherm established with X_a^* for models: (a) Ono-Kondo, (b) numerical, and (c) analytical.

For hard molecules, the number of adsorbed molecules plus number of vacant sites equals to total number of adsorption sites. Therefore, the density of vacancies plus density of adsorbed molecules equals 1:

$$X_a + X_v = 1 \tag{22}$$

Figure 9 shows relationship between density of vacancies and density of adsorbed molecules (a) Ono-Kondo, (b) numerical, and (c) analytical.

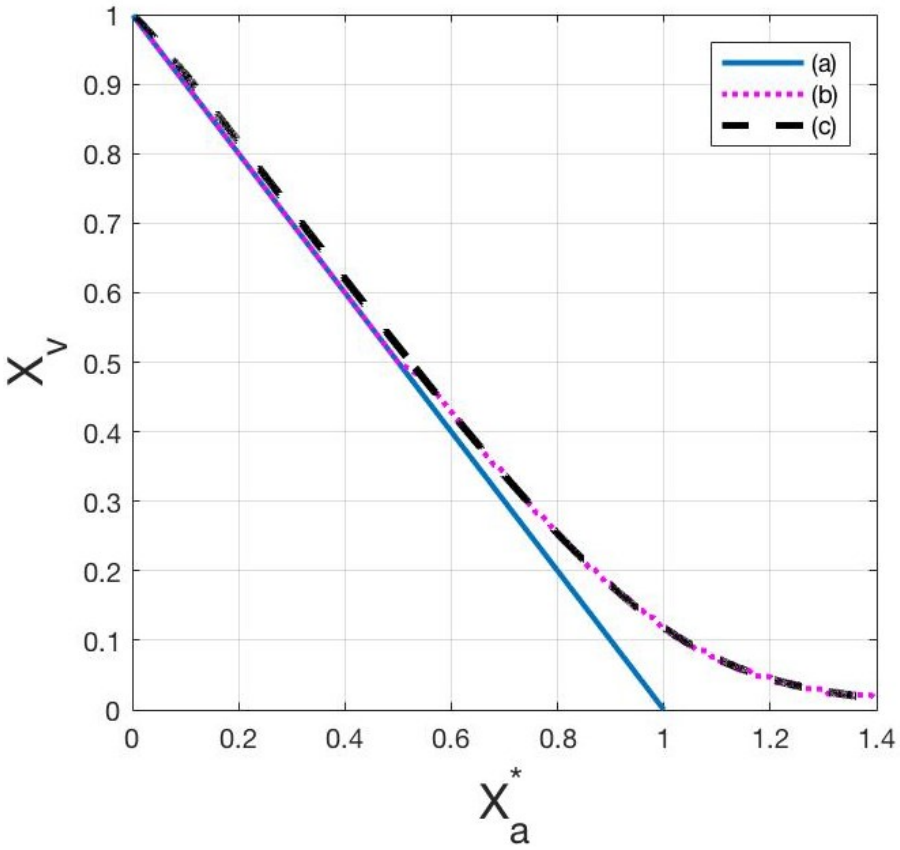

Figure 9. Relation between density of vacancies and density of adsorbed molecules: (a) Ono-Kondo, (b) numerical, and (c) analytical.

Figure 10 shows the internal energy, ΔU, as a function of X_a and X_a^*. As illustrated in Figure 10, the internal energy is lower than zero until (a) X_a reaches 0.98, or (b) X_a^* reaches 1.40, which means that adding adsorbate is favorable while the total number of sites is lower than 140% of its initial sites. Meanwhile, the lowest internal energy appears at $X_a^* = 0.90$. As X_a^* exceeds 0.90, the distance between two adsorbate molecules goes down and the adsorbate-adsorbate force turns into a repulsive force.

Figure 11 demonstrates simulation of adsorption isotherms for various φ_s/kT: (a) -3.0, (b) -5.0, and (c) -10.0. As attractive adsorbate-surface energy gets stronger, density of adsorbate on the surface, X_a, goes to unity more quickly.

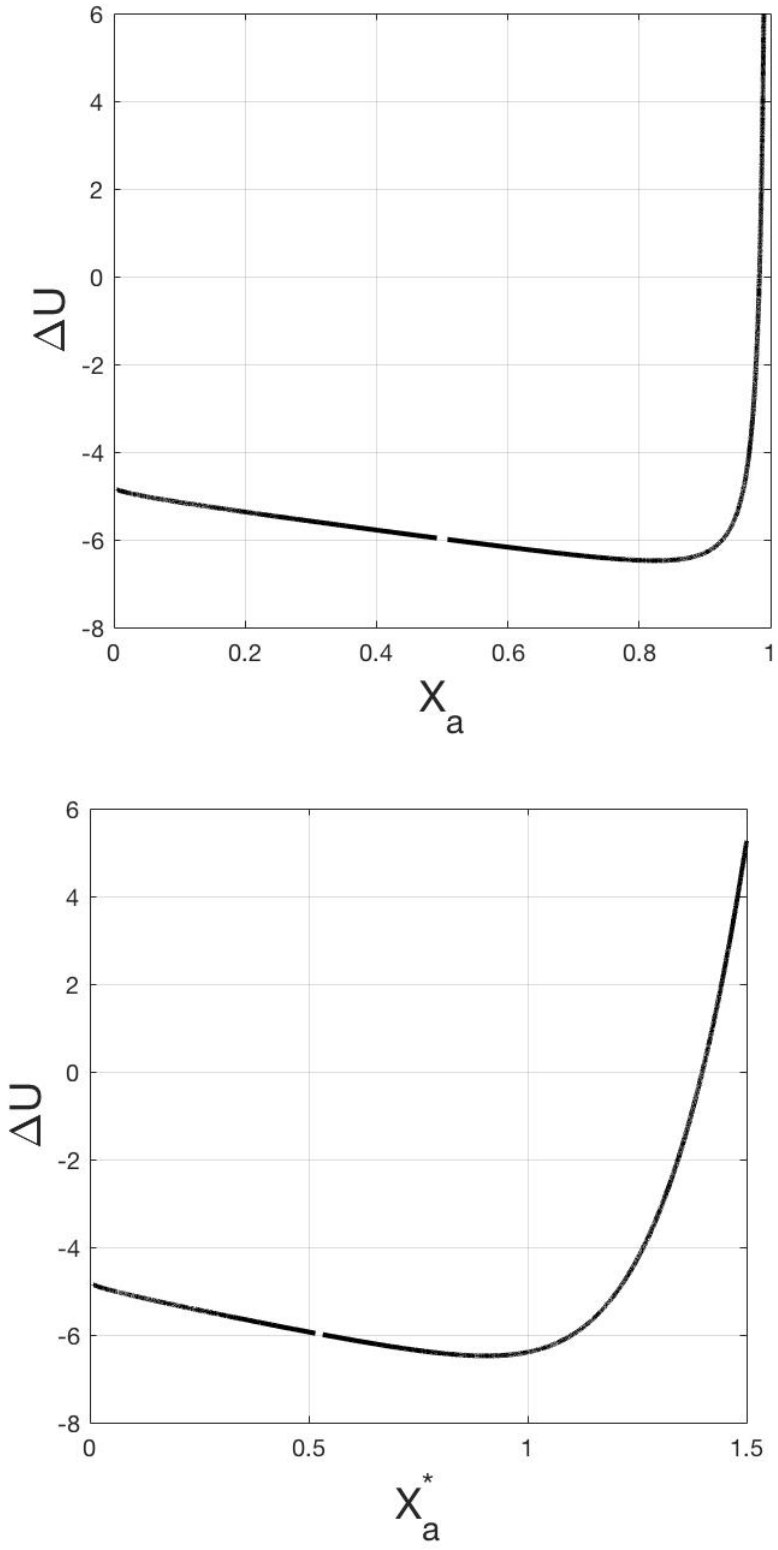

Figure 10. ΔU as a function of X_a (a) and X_a^* (b).

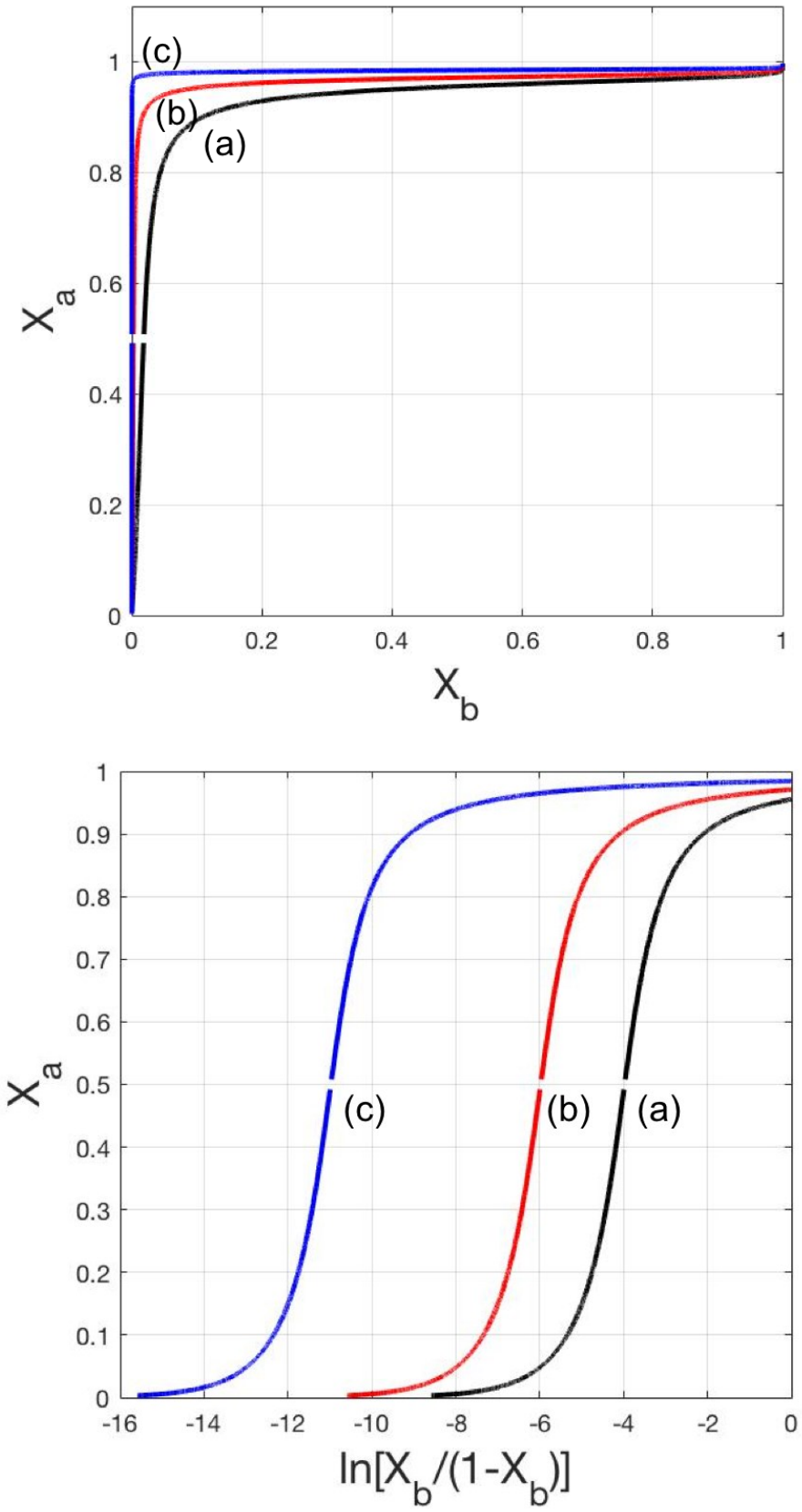

Figure 11. Adsorption isotherm for various φ_s/kT: (a) -3.0, (b) -5.0, and (c) -10.0.

Figure 12 shows the same variation of adsorbate-surface energy with respect to X_a^*, which can exceed unity since it is normalized to the initial number of sites. With stronger adsorbate-surface energy and the same bulk density, more molecules are adsorbed onto the surface, which is, X_a^* has a higher value under same bulk density. If we look at $X_a^* = 1.4$, which is, the total number of adsorbate molecules is 140% of the total number the initial site, the adsorption isotherm with (c) φ_s/kT equals to -10.0 can reach this number when bulk density is about only 0.22, whereas, the adsorption isotherm with (b) φ_s/kT equals to -5.0 will have to be 0.98 to reach this number, and the adsorption isotherm with (a) φ_s/kT equals to -3.0 will never reach this number before bulk density is fairly close to unity.

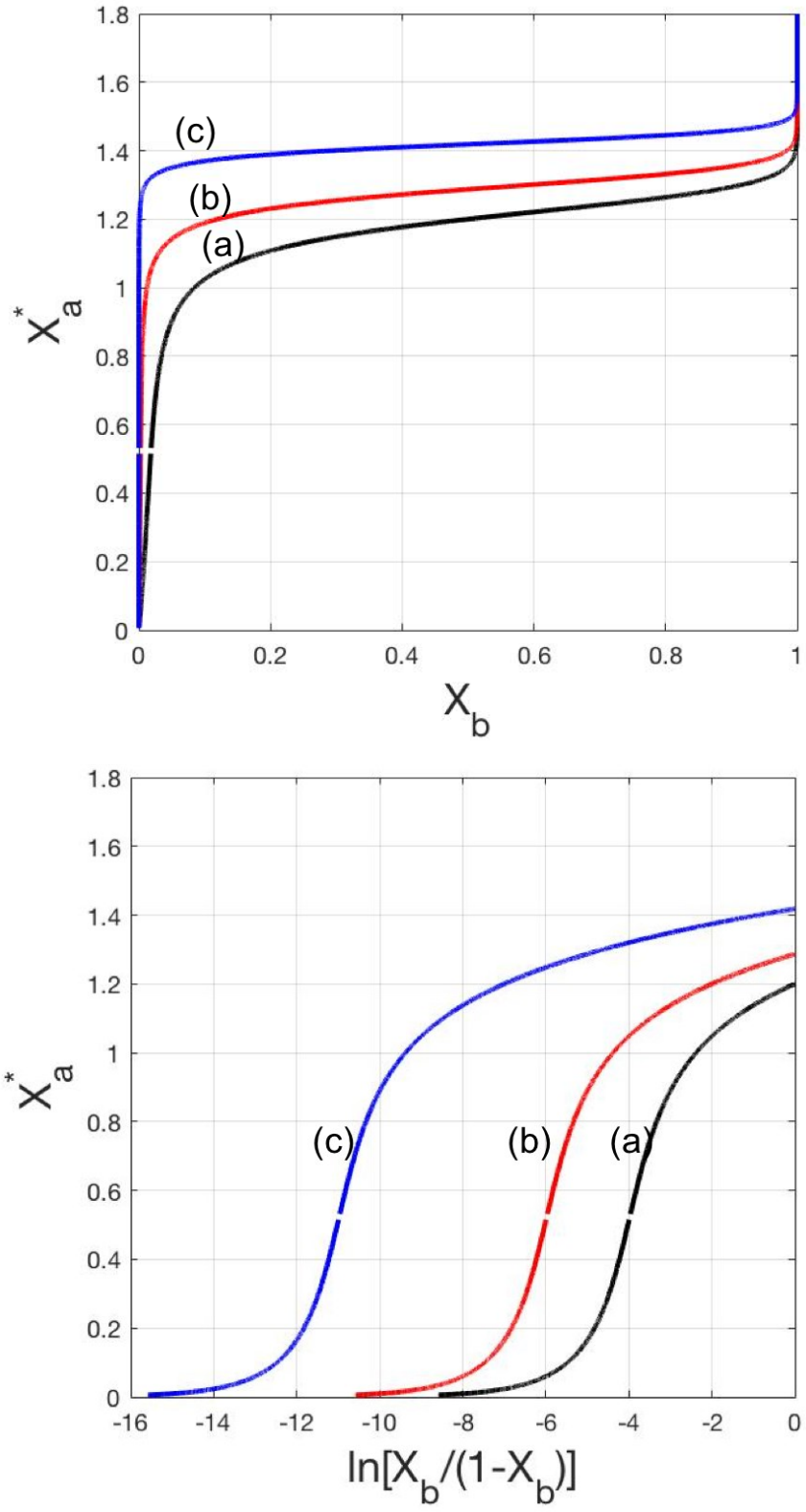

Figure 12. Adsorption isotherm for various φ_s/kT: (a) -3.0, (b) -5.0, and (c) -10.0 with respect to X_a^*.

The results for the analytical model show a gap in the curve when X_a approaches 0.5, as illustrated in Figures 10-12. This gap is caused by step size in variation of q. From analysis of equation (19), it follows that the number of decimals of q influences the final result of X_a. In this study, one step of q is one ten thousandth. This gives the X_{a_1}, closest to 0.5, a value of 0.5080.

3. Checkerboard Theory with Adsorption Compression

Checkerboard

Checkerboard, an 8x8 board used for the games of chess and checkers, contains a pattern of alternating dark and light color, often black and white, as shown in Figure 13(b). For a matrix of size m rows and n columns, the function of the board pattern would be as follows,

$$f(m,n) = \begin{cases} dark, if\ \ m\ \ is\ \ odd\ \ and\ \ n\ \ is\ \ odd \\ dark, if\ \ m\ \ is\ \ even\ \ \ and\ \ n\ \ is\ \ even \\ light, if\ \ m\ \ is\ \ even\ \ and\ \ n\ \ is\ \ odd \\ light, if\ \ m\ \ is\ \ odd\ \ and\ \ n\ \ is\ \ even \end{cases}$$

(23)

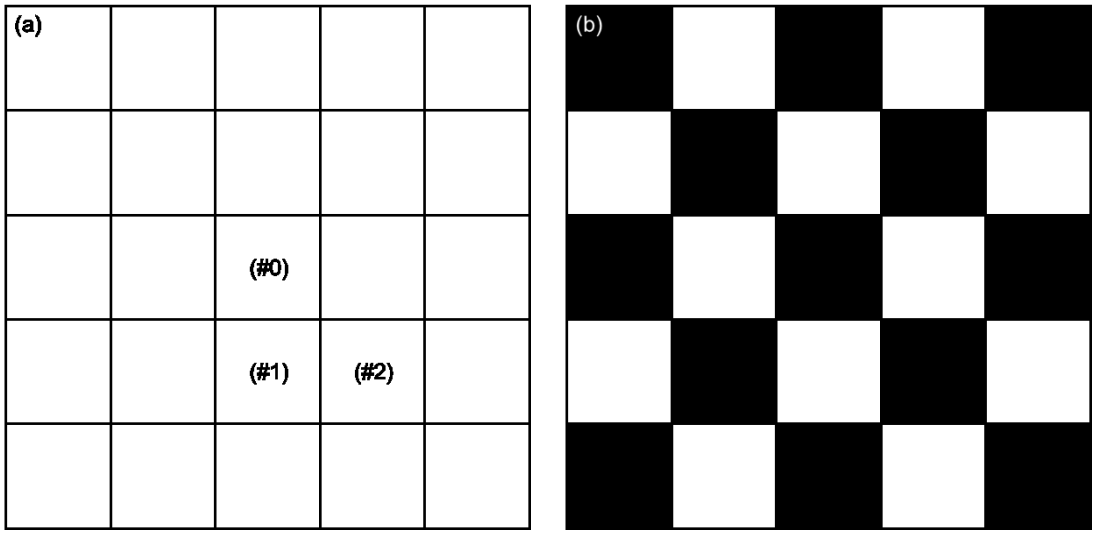

Figure 13. Fixed adsorption sites (a) and checkerboard (b).

Adsorption on Fixed Square Lattice

In the previous section, we talked about adsorption with soft molecules on a homogeneous flat surface without specific lattice sites. This allows the adsorption capacity to go above unity with regards to initial adsorption capacity ($X_a^* > 1$). Here, we consider fixed adsorption sites with a square lattice structure, as illustrated in Figure 13(a).

Consider two situations -- first, with the adsorbate molecular diameter smaller than the distance between two sites [the side length of a single square in Figure 13(a)], shown in Figure 14(a), the relationship of two adsorbate molecules and adsorption surface can be imagined in Figure 3(a), where compression never appears and adsorbate molecules can barely affect the location of each other. The second case is when the diameter of adsorbate molecule is greater than the distance between two sites, which makes the black molecule in Figure 14(b) unable to be adsorbed without distortion. In this situation, the location of the adsorbate molecules that are already adsorbed on the surface would significantly affect the location of the molecules adsorbing subsequently.

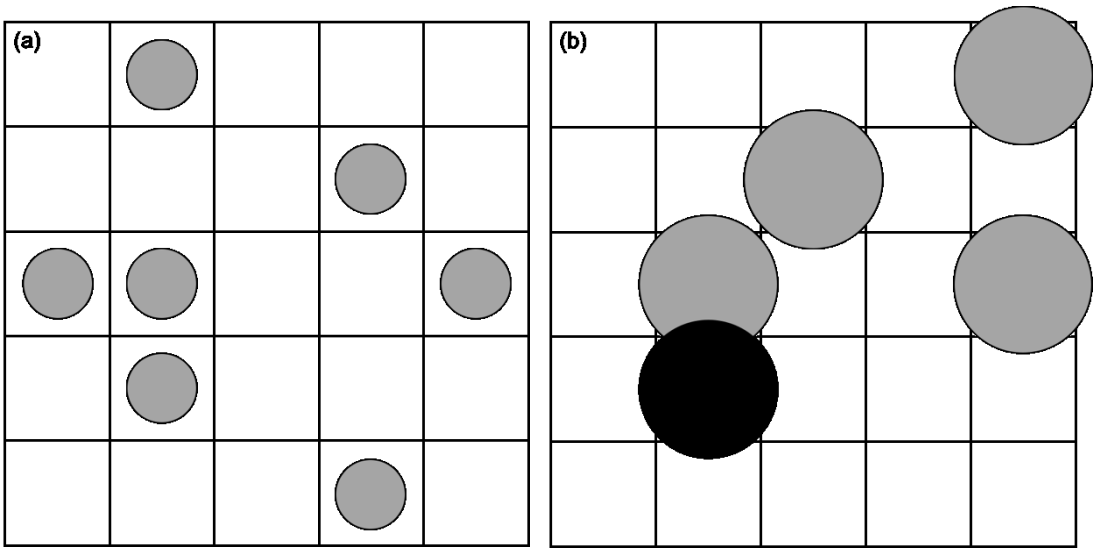

Figure 14. Adsorbate molecules at $(\sigma/d) < 1$ (a), and at $(\sigma/d) > 1$ (b).

If the spacing of the lattice is unity, the length between site (#0) and site (#1) in Figure 13(a) would also be unity, and length between site (#0) and site (#2) would be $\sqrt{2}$. In terms of parameters of Lennard-Jones potential, this indicates that $1 < (\sigma/d) < \sqrt{2}$, if two molecules are adsorbed on sites (#0) and (#1). Obviously, these molecules repel each other. If two molecules are adsorbed on sites (#0) and (#2), they would attract each other as long as $(\sigma/d) < \sqrt{2}$.

Checkerboard Theory

To understand adsorption compression in lattice system, we have developed a checkerboard theory with the following assumptions:

- molecules sit on sites of the square lattice;

- adsorbate molecules form a monolayer;

- energy of interaction between adsorbent surface and an adsorbate molecule is φ_s/kT;

- energy of interaction between adsorbate molecules is described by Lennard-Jones potential function with the distance between adsorbed molecules being d. When $d/\sigma > 1$, the molecules are attracted to each other; When $d/\sigma < 1$, neighboring adsorbate molecules repel each other;

- energy of interaction between adsorbate molecules in the bulk is φ_b/kT;

Consider a central site, which is the black dot in Figure 15. The eight sites surrounding the central site are divided into two groups, 1st nearest neighbor and 2nd nearest neighbor, as (1)s and (2)s in Figure 15. For case (b) on Figure 14, $(d/\sigma) < 1$. Here we assume boundary conditions around the central cluster shown in Figure 15.

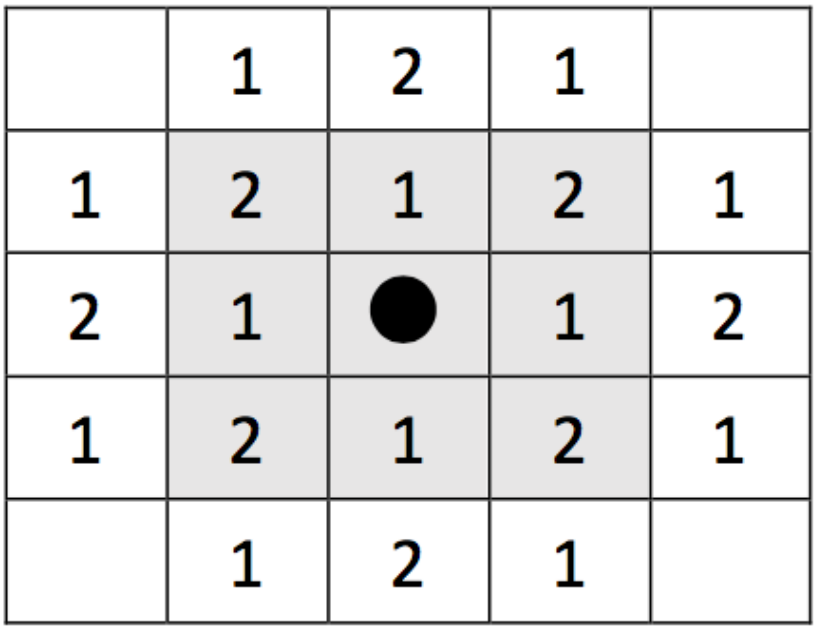

Figure 15. Adsorption sites of a central cluster: central site (black dot), 1st nearest neighbors (1), and 2nd nearest neighbors (2).

Consider the situation where the central site is occupied by an adsorbate molecule. Under this condition, the probability of having an adsorbate molecule on one of the 1st nearest neighbor sites is ρ_1'. On the other hand, let ρ_1'' be the probability to have an adsorbate molecule on a 1st nearest neighbor site when the central site is vacant. Then, the probability of having the 1st nearest neighbor site occupied, ρ_1, can be calculated as follows,

$$\rho_1 = \rho_1'\rho_2 + \rho_1''(1-\rho_2) \tag{24}$$

where ρ_2 is the probability to have 2nd nearest neighbor site occupied.

Equation (7) can be written for sites 1 and 2 which gives the following equations for ρ_1', ρ_1'', and ρ_2:

$$\begin{cases} \ln\frac{\rho_1'(1-\rho_\mathrm{b})}{\rho_\mathrm{b}(1-\rho_1')} + 3\rho_2\frac{\varphi}{kT} + \frac{\varphi}{kT} + \frac{\varphi_s}{kT} - 5\rho_\mathrm{b}\frac{\varphi_b}{kT} = 0 \\ \ln\frac{\rho_1''(1-\rho_\mathrm{b})}{\rho_\mathrm{b}(1-\rho_1'')} + 3\rho_2\frac{\varphi}{kT} + \frac{\varphi_s}{kT} - 5\rho_\mathrm{b}\frac{\varphi_b}{kT} = 0 \\ \ln\frac{\rho_2(1-\rho_\mathrm{b})}{\rho_\mathrm{b}(1-\rho_2)} + 4\rho_1\frac{\varphi}{kT} + \frac{\varphi_s}{kT} - 5\rho_\mathrm{b}\frac{\varphi_b}{kT} = 0 \end{cases}$$

(25)

where ρ_b is the bulk density, φ/kT is the energy of adsorbate-adsorbate interactions, and φ_b/kT is the energy of interaction between molecules in the bulk.

Results and Discussions

Equations (24) and (25) have four unknowns, ρ_1, ρ_2, ρ_1', and ρ_1''. Here we performed calculations for $\varphi_s/kT = -5.0$, $\epsilon_o/kT = 0.5$, and for φ/kT determined by equation (3). We have solved these equations with various σ/d from 1.01 to 1.10. Figure 16 shows ρ_1 [line (I)], ρ_2 [line (II)], ρ_1' [line (III)], and ρ_1'' [line (IV)] as functions of the bulk density. If σ/d is close to unity, the adsorbate molecules are slightly larger than the distance between two neighboring sites. Then, the 1st nearest neighbor site is more favorable than the 2nd nearest neighbor site. In this case, the ρ_1' and ρ_1'' curves are almost identical. As σ/d increases, the difference between ρ_1'

and ρ_1'' becomes more significant, because occupancy of the central site has an impact on the 1st nearest neighbor sites. In particular, having an adsorbate molecule on the central site always makes adsorption on the 1st neighbor site more difficult. When $d/\sigma < 1$, Tables 1 and 2 shows the relationship between σ/d and d/σ.

σ/d	d/σ
0.89	2^(1/6)
1.00	1.00000
1.01	0.99010
1.02	0.98039
1.03	0.97087
1.04	0.96154
1.05	0.95238
1.06	0.94340
1.07	0.93458
1.08	0.92593
1.09	0.91743
1.10	0.90909
1.11	0.90090
1.12	0.89286

Table 1. Comparison of σ/d and d/σ

As shown by Figure 16(e) and 16(f), at σ/d smaller than 1.05, ρ_1 dominates over ρ_2, because adsorptions on 1st nearest neighbor sites are more favorable. When σ/d exceeds 1.06, ρ_2 dominates, because the 2nd nearest neighbor sites are more favorable. While ρ_1' curve drops dramatically when σ/d exceeds 1.06, the difference between ρ_1' and ρ_1'' is still essential. When bulk density is 0.5 at $(\sigma/d) = 1.07$, ρ_1'' is 0.36 while $\rho_1' = 0.11$. This difference gradually vanishes when σ/d gets higher; this is because occupancy of the 2nd nearest neighbor sites affects both ρ_1' and ρ_1'' when adsorbate molecules are much larger than the distance between adsorption sites.

When ρ_2 is 0.9, the neighboring density is $\rho_1' = (1 + 0.9 \times 3)/4 = 0.925$, while $\rho_1'' = (0 + 0.9 \times 3)/4 = 0.675$.

As follows from Figure 16(j), at $(\sigma/d) = 1.10$, both ρ_1' and ρ_1'' are small except when the bulk density is close to unity.

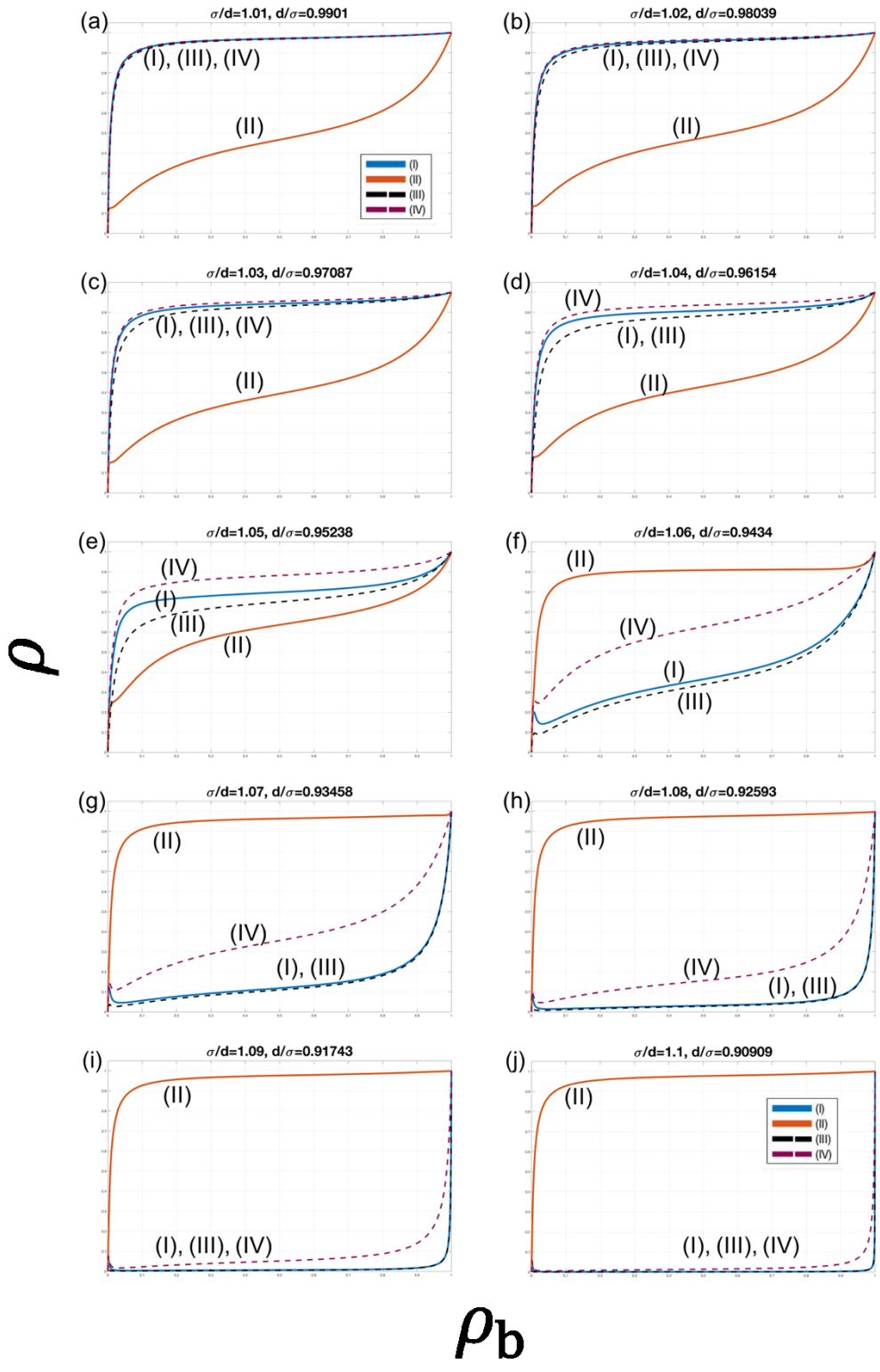

Figure 16. Dependence of ρ_1 (I), ρ_2 (II), ρ_1' (III), and ρ_1'' (IV) on ρ_b at various σ/d: (a)1.01, (b)1.02, (c)1.03, (d)1.04, (e)1.05, (f)1.06, (g)1.07, (h)1.08, (i)1.09, and (j)1.10 and $\varphi_s/kT = -5.0$.

Equation (25) can be written in the following form:

$$\begin{cases} \ln\frac{\rho_1'(1-\rho_b)}{\rho_b(1-\rho_1')} = -(3\rho_2\frac{\varphi}{kT} + \frac{\varphi}{kT} + \frac{\varphi_s}{kT} - 5\rho_b\frac{\varphi_b}{kT}) \\ \ln\frac{\rho_1''(1-\rho_b)}{\rho_b(1-\rho_1'')} = -(3\rho_2\frac{\varphi}{kT} + \frac{\varphi_s}{kT} - 5\rho_b\frac{\varphi_b}{kT}) \\ \ln\frac{\rho_2(1-\rho_b)}{\rho_b(1-\rho_2)} = -(4\rho_1\frac{\varphi}{kT} + \frac{\varphi_s}{kT} - 5\rho_b\frac{\varphi_b}{kT}) \end{cases}$$

(26)

Figure 17 shows dependence of ρ_1 (I), ρ_2 (II), ρ_1' (III), ρ_1'' (IV) and right-hand-side of equation (26) on ρ_b at various σ/d: (a)1.051, (b)1.052, (c)1.053, (d)1.054, (e)1.055. Table 2 gives comparison of σ/d and d/σ in this range of σ/d.

σ/d	d/σ
1.051	0.95147
1.052	0.95057
1.053	0.94967
1.054	0.94877
1.055	0.94787

Table 2. Comparison of σ/d and d/σ

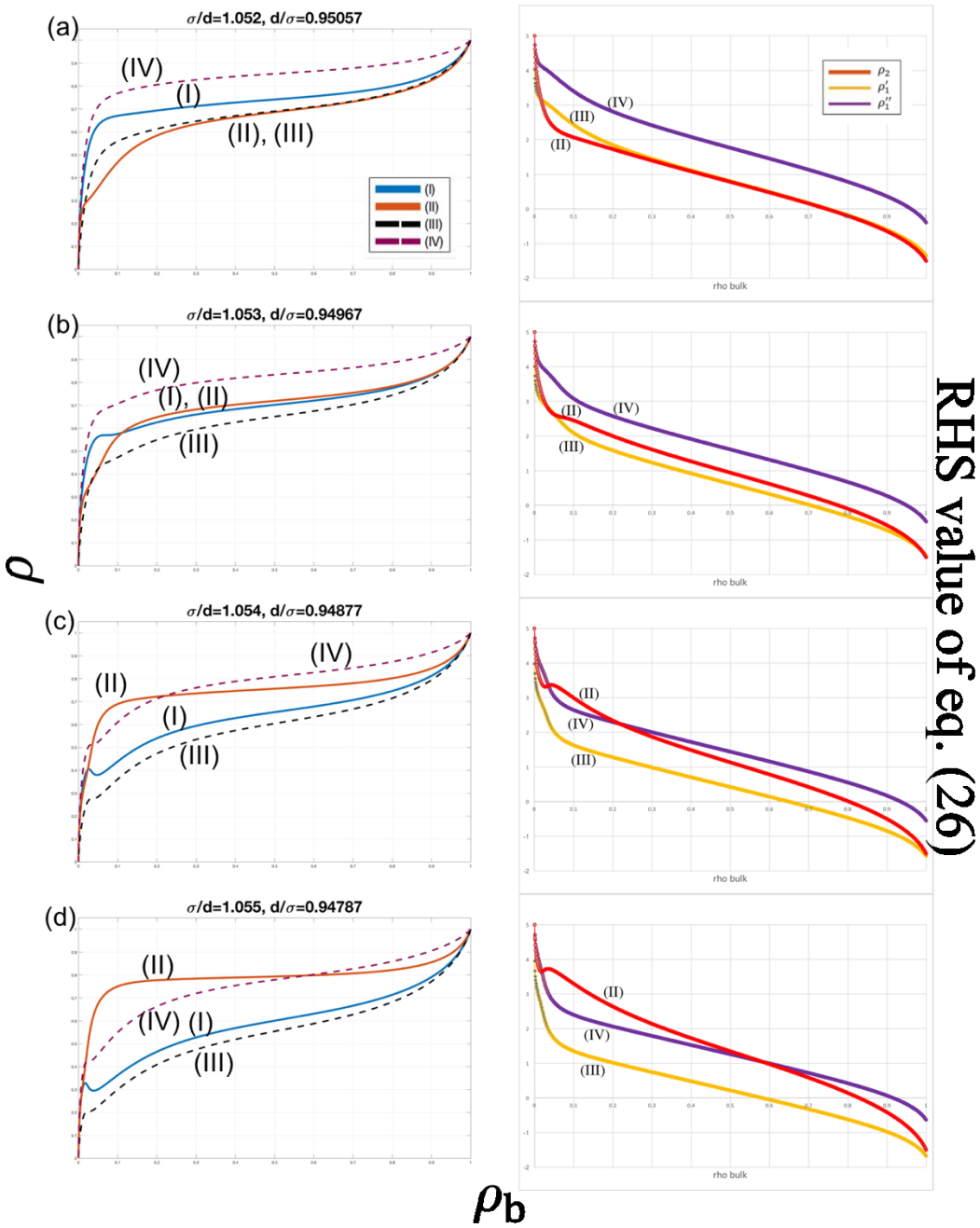

Figure 17. Dependence of ρ_1 (I), ρ_2 (II), ρ_1' (III), and ρ_1'' (IV) and right-hand-side of equation (26) on ρ_b at various σ/d: (a)1.052, (b)1.053, (c)1.054, (d)1.055.

When the values of RHS of equation (26) are zeros, values of ρ_2, ρ_1', or ρ_1'' are equal to the bulk density. For example, the first equation becomes:

$$\ln\frac{\rho_b}{(1-\rho_b)} = \ln\frac{\rho_1'}{(1-\rho_1')} \tag{27}$$

If RHS value of equation (26) is larger than zero, the values of ρ_2, ρ_1', or ρ_1'' are higher than the bulk density. This indicates that adsorbate molecules are more favorable to stay on adsorption sites than stay in the bulk. Figure 18 illustrates this: Figure 18 is Figure 17(c) with an auxiliary line (gray) with function: $x - y = 0$. No matter it is ρ_1, ρ_2, ρ_1', or ρ_1'', if ρ is lower than the auxiliary line, the bulk density is higher than ρ; therefore, adsorbate molecules tend to stay in the bulk, i.e. there is negative absolute adsorption.

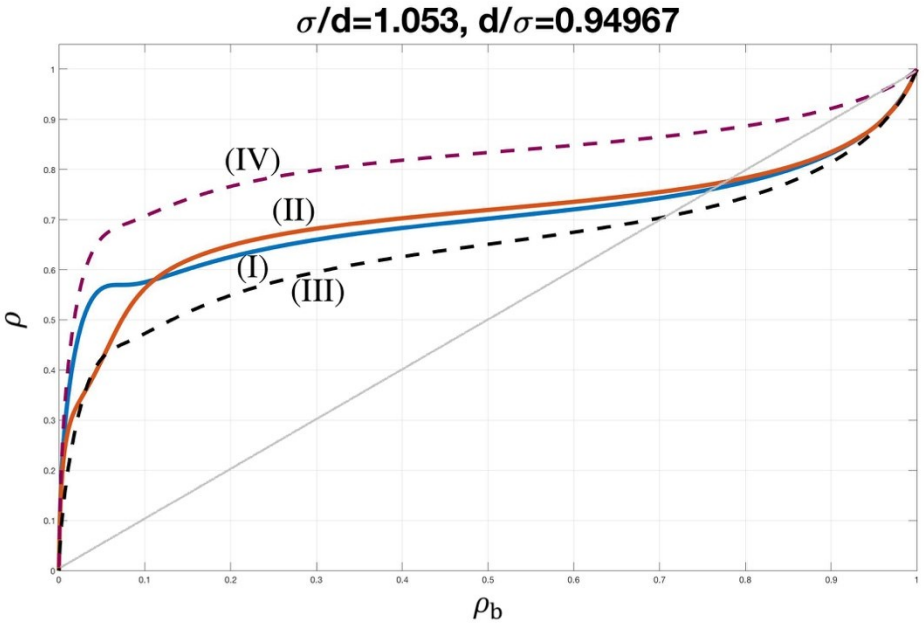

Figure 18. Dependence of ρ_1 (I), ρ_2 (II), ρ_1' (III), and ρ_1'' (IV) on ρ_b with an auxiliary line ($x - y = 0$) at $(\sigma/d) = 1.053$.

Figure 19 shows the dependence of (I) ρ_1, (II) ρ_2, (III) ρ_1', and (IV) ρ_1'' on the bulk density for various σ/d: (a) 1.02, (b) 1.04, (c) 1.06, (d) 1.08, and (e) 1.10. As shown by Figure 19, the trends of ρ_1' and ρ_1'' are similar. However, ρ_1 and ρ_2 show the opposite trend: as σ/d goes up, ρ_1 goes down while ρ_2 goes up.

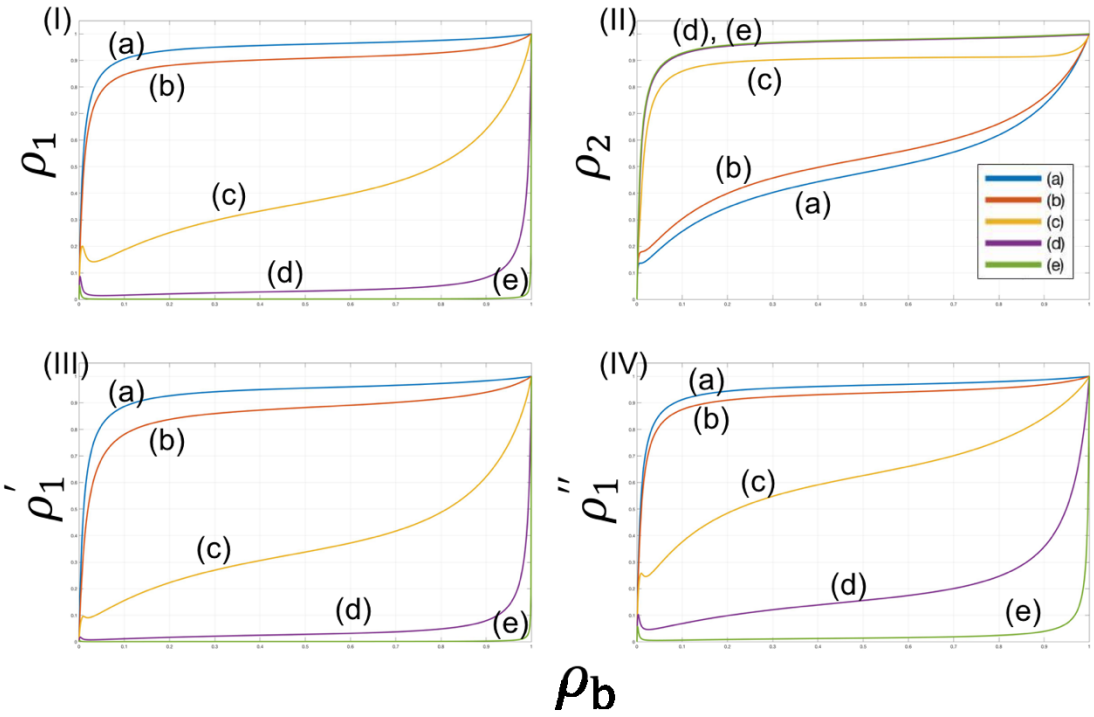

Figure 19. Dependence of (I) ρ_1, (II) ρ_2, (III) ρ_1', and (IV) ρ_1'' on the bulk density for various σ/d: (a) 1.02, (b) 1.04, (c) 1.06, (d) 1.08, and (e) 1.10.

Figure 20 shows the dependence of ρ_1 (I), ρ_2 (II), ρ_1' (III), and ρ_1'' (IV) on the bulk density for $(\varphi_s/kT) = -3.0$ at various σ/d: (a)1.01, (b)1.02, (c)1.03, (d)1.04,

(e)1.05, (f)1.06, (g)1.07, (h)1.08, (i)1.09, and (j)1.10. Figure 21 shows dependence of ρ_1 (I), ρ_2 (II), ρ_1' (III), and ρ_1'' (IV) on the bulk density for $(\varphi_s/kT) = -10.0$ at various σ/d: (a)1.01, (b)1.02, (c)1.03, (d)1.04, (e)1.05, (f)1.06, (g)1.07, (h)1.08, (i)1.09, and (j)1.10.

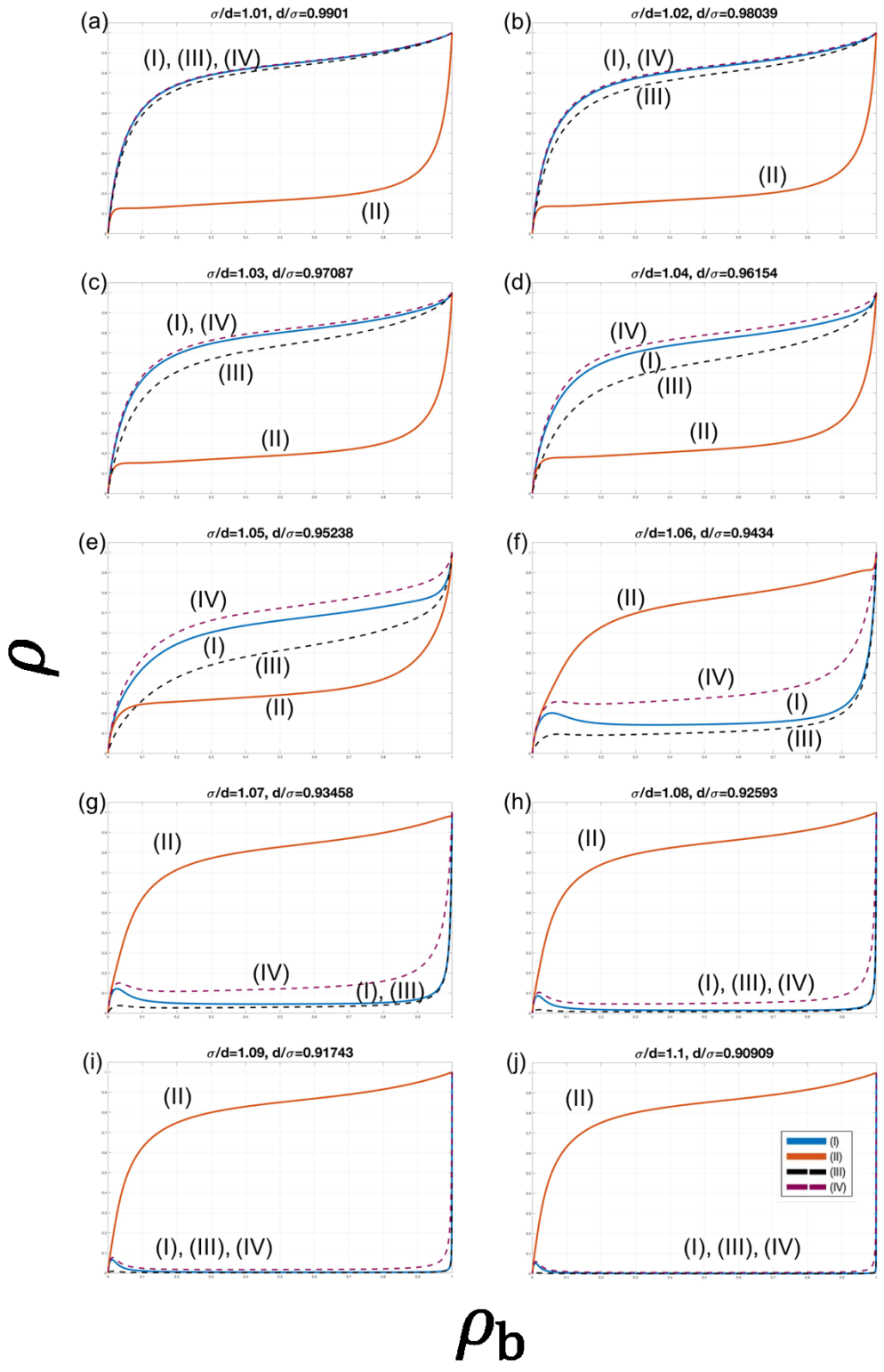

Figure 20. Dependence of ρ_1 (I), ρ_2 (II), ρ_1' (III), and ρ_1'' (IV) on the bulk density for $(\varphi_s/kT) = -3.0$ at various σ/d: (a)1.01, (b)1.02, (c)1.03, (d)1.04, (e)1.05, (f)1.06, (g)1.07, (h)1.08, (i)1.09, and (j)1.10.

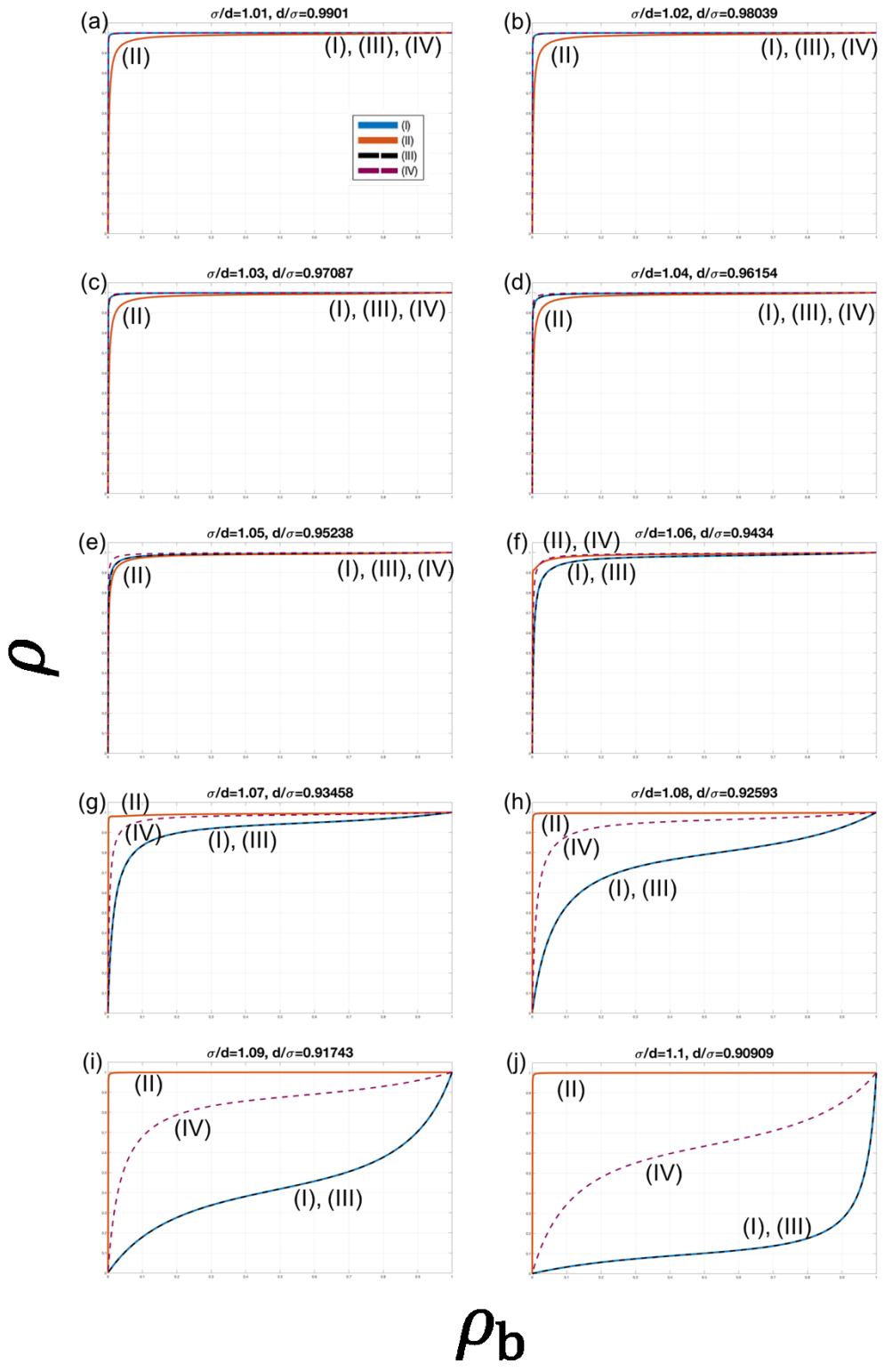

Figure 21. Dependence of ρ_1 (I), ρ_2 (II), ρ_1' (III), and ρ_1'' (IV) on the bulk density for $(\varphi_s/kT) = -10.0$ at various σ/d: (a)1.01, (b)1.02, (c)1.03, (d)1.04, (e)1.05, (f)1.06, (g)1.07, (h)1.08, (i)1.09, and (j)1.10.

Figure 22 shows dependence of ρ_1 (a, c, e) (solid lines) and ρ_2 (b, d, f) (dashed lines) on the bulk density for $\sigma/d =$ 1.05 (I) and 1.06 (II), and different φ_s/kT: -3.0 (a, b), -5.0 (c, d), and -10.0 (e, f). Figure 23 shows the average density as a function of the bulk density for φ_s/kT: -3.0 (I), -5.0 (II), and -10.0 (III) at various σ/d: (a) $2^{-1/6}$, (b) 1.00, (c) 1.05, (d) 1.06, (e) 1.07, (f) 1.08, (g) 1.09, and (h) 1.10.

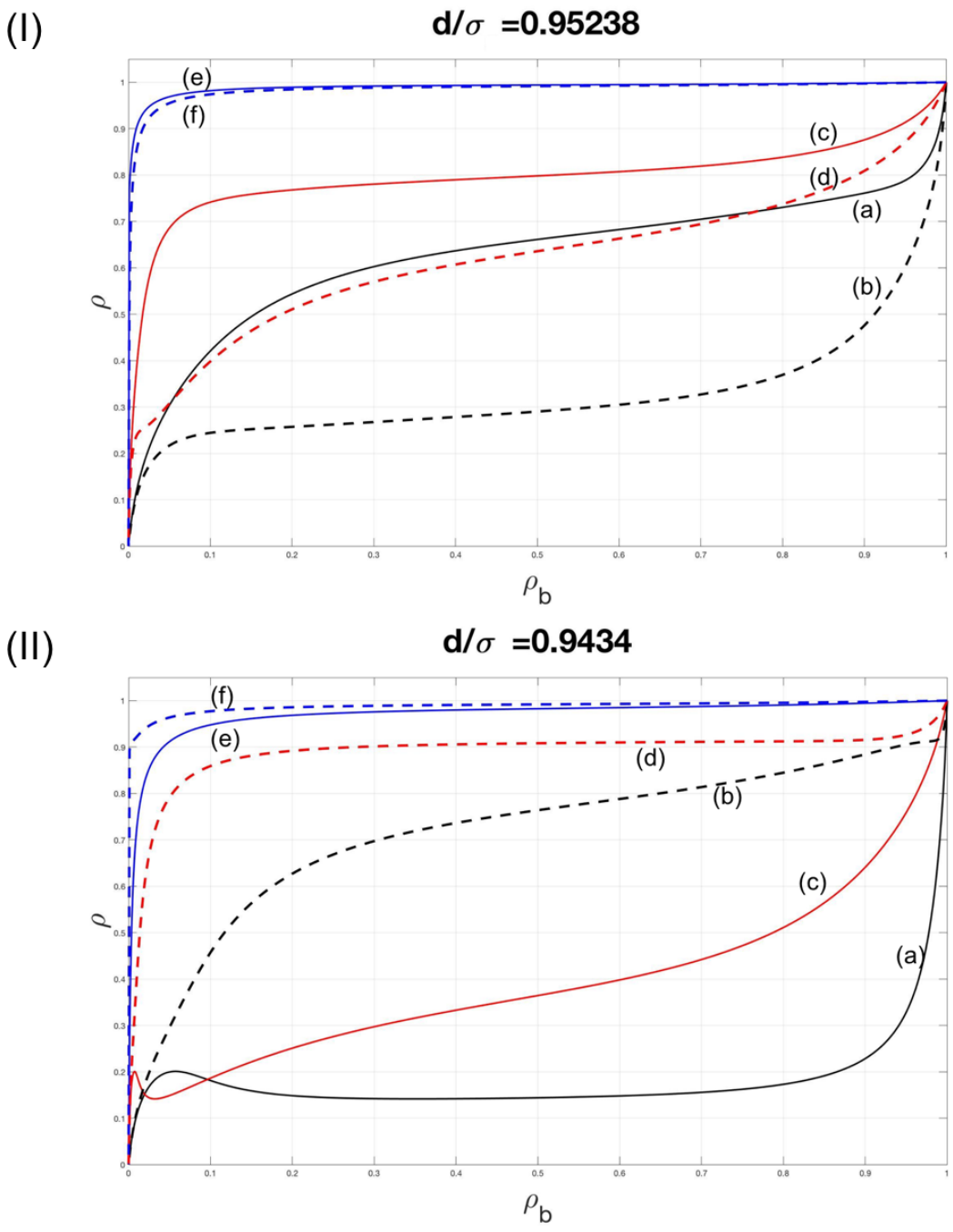

Figure 22. Dependence of ρ_1 (a, c, e) (solid lines) and ρ_2 (b, d, f) (dashed lines) on the bulk density for $\sigma/d =$ 1.05 (I) and 1.06 (II), and different φ_s/kT: -3.0 (a, b), -5.0 (c, d), and -10.0 (e, f).

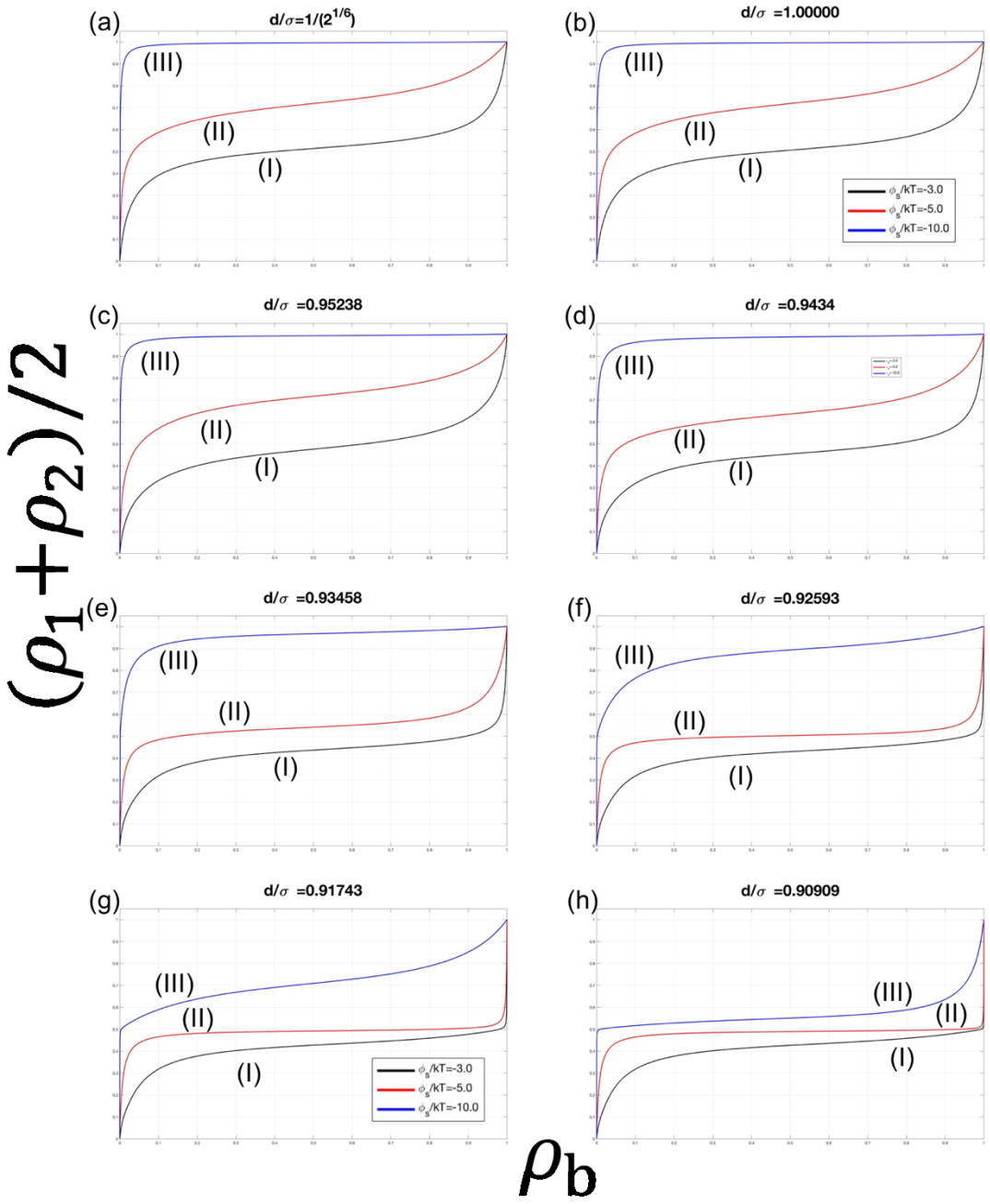

Figure 23. The average density as a function of the bulk density for φ_s/kT: -3.0 (I), -5.0 (II), and -10.0 (III) at various σ/d: (a) $2^{-1/6}$, (b) 1.00, (c) 1.05, (d) 1.06, (e) 1.07, (f) 1.08, (g) 1.09, and (h) 1.10.

Conclusion

Adsorption compression happens when the surface of a solid has a high affinity to adsorbing molecules. The force field of this system draws the adsorbing molecules onto the surface strongly at a density higher than in a normal liquid. Adsorption compression keeps happening until the loss in free energy due to attraction between adsorbate and surface is compensated by the gain in free energy due to repulsion between adsorbates. This paper illustrates a general idea of adsorption isotherm for systems with adsorption compression from both analytical and numerical methods. Equations are built to monitor adsorption compression of many kinds of molecules as long as the parameters, such as σ, ϵ_o/kT, and φ_s/kT, are determined.

Checkerboard theory for adsorption compression is a simple model with a good correlation of repulsion on a monolayer adsorbent surface. Due to the simplicity, it has its limitation such as some assumptions are different between equations. Despite of the minor flaws, this model is still a good approach of reducing the sophistication in adsorption compression.

References

1. Crini, Grégorio, and Pierre-Marie Badot, eds. *Sorption processes and pollution: Conventional and non-conventional sorbents for pollutant removal from wastewaters*. Presses Univ. Franche-Comté, 2010.

2. McNaught, Alan D., and Alan D. McNaught. *Compendium of chemical terminology*. Vol. 1669. Oxford: Blackwell Science, 1997.

3. Calvert, Jack George. "Glossary of atmospheric chemistry terms (Recommendations 1990)." *Pure and applied chemistry*62.11 (1990): 2167-2219.

4. Langmuir, I. *J. Am. Chem. Soc.* **1916**, *38*, 2221

5. Frumkin, A. N. "Surface tension curves of higher fatty acids and the equation of condition of the surface layer." *Z. phys. Chem* 116 (1925): 466-484.

6. Guggenheim, E. A., and R. H. Fowler. "Statistical thermodynamics." *pp. 422ff, Cambridge University Press, London* (1949).

7. Brunauer, Stephen, P. H. Emmet, and F. Teller. "Surface area measurements of activated carbons, silica gel and other adsorbents." *J. Am. Chem. Soc* 60 (1938): 309-319.

8. Lennard-Jones, J. E. In *The Adsorption of Gases by Solids*; Faraday Society: London, 1932; p333. London, F. *Z. Phys. Chem.***1930**,*11*,222.

9. Polanyi, Michael. "Adsorption from the point of view of the Third Law of Thermodynamics." *Verh. Deut. Phys. Ges* 16 (1914): 1012-1016.

10. Hill, T. L. Theory of Physical Adsorption. *Adv. Catal.* **1948- 1952**, *4*, 211-255.

11. Nicholson, David. *Computer simulation and the statistical mechanics of adsorption*. Academic Press, 1982.

12. Steele, W. A. *Interaction of Gases with Solid Surfaces*; Pergamon Press: Oxford, 1974.

13. Nicholson, D. *J. Chem. S oc., Faraday T rans. 1* **1996**, *92*, 1-9.

14. Ono, S.; Kondo, S. Molecular Theory of Surface Tension in Liquids. In *Encyclopedia of Physics*; Flügge, S., Ed.; Springer: Berlin, 1960; Vol. 10, p 134.

15. Aranovich, G. L., and M. D. Donohue. "New approximate solutions to the Ising problem in three dimensions." *Physica A: Statistical Mechanics and its Applications* 242.3-4 (1997): 409-422.

16. Aranovich, Grigoriy, and Marc Donohue. "Analysis of adsorption isotherms: Lattice theory predictions, classification of isotherms for gas–solid equilibria, and similarities in gas and liquid adsorption behavior." *Journal of colloid and interface science* 200.2 (1998): 273-290.

17. Aranovich, G. L., and M. D. Donohue. "Phase loops in density-functional-theory calculations of adsorption in nanoscale pores." *Physical Review E*60.5 (1999): 5552.

18. Aranovich, G. L., and M. D. Donohue. "Lattice density functional theory predictions of order–disorder phase transitions." *The Journal of Chemical Physics* 112.5 (2000): 2361-2366.

19. Aranovich, G. L., and M. D. Donohue. "Surface compression in adsorption systems." *Colloids and Surfaces A: Physicochemical and Engineering Aspects* 187 (2001): 95-108.

20. Rice, S. A., J. Gryko, and U. Mohanty. "Fluid Interfacial Phenomena." *John Wiley & Sons Ltd* (1986): 255-342.

21. Rittner, F., et al. "Adsorption of nitrogen on rutile (110): Monte Carlo computer simulations." *Langmuir* 15.4 (1999): 1456-1462.

22. D'Evelyn, M. P.; Rice, S. A. *Phys. Rev. Lett.* **1982**, *47*, 1844; *Discuss. Faraday S oc.* **1982**, *16*, 71; *J . Chem . Phys.* **1983**, *78*, 5081; *J . Chem . Phys.* **1983**, *78*, 5225.

23. Heuberger, M.; Zach, M.; Spenser, N.D.*Science***2001**,*292*,905.

24. Israelachvili, Jacob, and Delphine Gourdon. "Putting liquids under molecular-scale confinement." *Science* 292.5518 (2001): 867-868.

25. Fairbrother, D. Howard, et al. "Structure of monolayer and multilayer magnesium chloride films grown on Pd (111)." *Langmuir* 13.7 (1997): 2090-2096.

26. Karnaukhov, A. P. "Improvement of methods for surface area determinations." *Journal of colloid and interface science* 103.2 (1985): 311-320.

27. Abaza, S., G. L. Aranovich, and M. D. Donohue. "Adsorption compression in surface layers." *Molecular Physics* 110.11-12 (2012): 1289-1298.

28. Jones, John Edward. "On the determination of molecular fields. II. From the equation of state of a gas." *Proceedings of the Royal Society of London A: Mathematical, Physical and Engineering Sciences*. Vol. 106. No. 738. The Royal Society, 1924.

29. Al-Sarraf, N., and D. A. King. "Calorimetric adsorption heats on low-index nickel surfaces." *Surface science* 307 (1994): 1-7.

30. Kose, Rickmer, Wendy A. Brown, and David A. King. "Role of lateral interactions in adsorption kinetics: CO/Rh {100}." *The Journal of Physical Chemistry B* 103.41 (1999): 8722-8725.

31. Molinari, Ettore, and Massimo Tomellini. "Chemisorption and the vibrational excitation of the adlayer." *Surface science*552.1-3 (2004): 180-192.

32. Ebner, C., Craig Rottman, and Michael Wortis. "Epitaxy and thick-film formation on an attractive substrate: The systematics of a lattice-gas model." *Physical Review B* 28.8 (1983): 4186.

33. Fairbrother, D. Howard, Joel G. Roberts, and Gabor A. Somorjai. "The growth of magnesium chloride monolayer and multilayer structures on different transition metal (Pt, Pd, Rh) single crystals with varied orientations." *Surface science* 399.1 (1998): 109-122.

34. Charniak, C. L., et al. "Monte Carlo simulations of phase transitions and adsorption isotherm discontinuities on surface compression." *Journal of colloid and interface science* 324.1-2 (2008): 9-14.

35. Wetzel, T. E., et al. "Monte Carlo simulations on the effect of substrate geometry on adsorption and compression." *The Journal of chemical physics* 120.24 (2004): 11765-11774.

36. Sumanatrakul, Panita, et al. "Adsorption Compression Analysis for Supercritical Fluids using Ono-Kondo Model." *Adsorption* 11.2 (2011): 45-52.

37. Lee, Lloyd L. Molecular thermodynamics of nonideal fluids. Butterworth-Heinemann, 2016.

38. Bier, Daniel S. *Expandable Monolayer Capacity for Modeling Adsorption Compression Systems*. Diss. Johns Hopkins University, 2016.

39. Aranovich, G. L., C. Sangwichien, and M. D. Donohue. "Intermolecular repulsions in adsorbed layers." *Journal of colloid and interface science* 227.2 (2000): 553-560.

Appendices

Matlab code for comparison of Ono-Kondo equation, analytic method and numeric method

```
clc
clear
tic; %elapsed time reporting

%constants-------------------------------------------------------------------
E = -0.5; %energy for interaction Ono-Kondo
Eo = E; %energy for interaction in bulk
Es = -5.0; %energy for interaction with surface
sigma = 3.5; %size parameter
z = 4; % # interactions with neighbors (lattice system)
ko = 1; % # interactions with surface
k1 = z; % # interactions with neighbors
k2 = 0.5;% # interactions in bulk
vo = 3.92862; %LJ minimum (V/E = -1)
p = 0; %initial # particle adsorbed (also being a counter for numeric)
num = 0; % # sites added counter, has potential to go up by 1 each time
Go = z; %LJ model constant, Go = 2*pi*go
K = 1; %packing factor (LJ model constant)
k = 1.38*10^-23; %unit:J/K
T = 298;         %unit:K

%parameters------------------------------------------------------------------
iRow = 10; %initial number of rolls
iCol = 10; %initial number of colums
area = iRow*iCol; %available volume for numeric solution
fRow = 0;
fCol = 0;
Nso = area; %initial # sites
Ns = Nso; % # sites for numeric, equals 100 initially
opt = []; %1 means no site added, 2 means site added, for numeric
xb_1 = []; %calculated bulk density
Vnu = []; % # vancancies for numeric
particle = []; % # particles adsorbed
r1 = []; %distance between particles for option 1
r2 = []; %distance between particles for option 2
Elj1=[]; %LJ energy for option 1 (superceded to -1 if P is too small)
Efinal = []; %Ea of option chosen
E1 = []; %Ea of option 1
E2 = []; %Ea of option 2


%Matrices--------------------------------------------------------------------
onokondo = []; %result for OK
analytic = []; %result for analytic
numeric = []; %result for numeric
lennard = []; %result for adsorption with lennard-jones


%Ono-Kondo-------------------------------------------------------------------
for i = 1:1000
Xaok = i/1000;
Eok = (Es)+(z*(E)*Xaok);

Xbok = Xaok/(Xaok+((1-Xaok)*exp(-Eok)));
Xvok = 1-Xaok;

onokondo(i,1) = Xaok;
onokondo(i,2) = Xbok;
onokondo(i,3) = Xvok;
end
```

```
%Analytic Solution-------------------------------------------------------
%Calculation of nso
q = 0.5;
Xac = real(0.5*(1+sqrt(1-1/(z*E*q*(2-5*q)))));
nsc = (q^(1/3))/(sigma^2);
Vc = nsc-(Xac*nsc);
ac = Xac*nsc;
slope = -1;
intersection = Vc-(slope*ac);
nso = intersection;

for h = 1:5000
q = 0.5 + (h)/1000;

if (z*(Eo)*q*(2-5*q)) > 1
ns = (q^(1/3))/(sigma^2);

Xaan1 = 0.5*(1+sqrt(1-(1/(z*(Eo)*q*(2-5*q)))));
Xaan2 = 0.5*(1-sqrt(1-(1/(z*(Eo)*q*(2-5*q)))));

Xban1 = Xaan1/(Xaan1+((1-Xaan1)*exp(-(Es+(4*z*Eo*q*(1-q)*Xaan1)))));
Xban2 = Xaan2/(Xaan2+((1-Xaan2)*exp(-(Es+(4*z*Eo*q*(1-q)*Xaan2)))));

analytic(h,1) = Xaan1;
analytic(h,2) = Xaan2;
analytic(h,3) = Xban1;
analytic(h,4) = Xban2;

V1 = ns-(Xaan1*ns);
V2 = ns-(Xaan2*ns);
a1 = Xaan1*ns;
a2 = Xaan2*ns;

analytic(h,7) = Xaan1*ns/nso; %Xa*
analytic(h,8) = Xaan2*ns/nso; %Xa*
analytic(h,9) = ns;
analytic(h,10) = V1;
analytic(h,11) = V2;
analytic(h,12) = a1;
analytic(h,13) = a2;

Xvan1 = (ns-a1)/ns;
Xvan2 = (ns-a2)/ns;

Rana = sqrt(1/ns);
Paa = z*Eo*(((sigma/Rana)^6)-((sigma/Rana)^12)); %Lennard-Jones potential
miu = Es+(4*z*Eo*a1*(((sigma^6)*(ns^2))-((sigma^12)*(ns^5))))+(log(a1/(ns-a1))*k*T);

analytic(h,5) = Xvan1;
analytic(h,6) = Xvan2;
analytic(h,14) = Rana; %r
analytic(h,15) = Paa/(-Eo); %Normalized Gamma (Lennard-Jones potential)
analytic(h,16) = Es+(4*z*Eo*a1*(((sigma^6)*(ns^2))-((sigma^12)...
    *(ns^5))))+(log(a1/(ns-a1))*k*T); % miu/kT
analytic(h,17) = Es+(4*Paa)+log(Xaan1/(1-Xaan1));
analytic(h,18) = exp(miu/Eo);
else
    continue
end
end

analytic(any(analytic,2)==0,:)=[]; %deletion if imaginary number occurs
```

```
125
126
127     %numeric-------------------------------------------------------------------
128 -   syms x y
129 -   xb1solve = [];
130 -   for j = 1:area*1.5
131 -   p = p+1; %particles adsorbed by 1
132
133     %option 1 (no site added)
134 -   Xanu1 = p/Ns;
135 -   r1 = vo/(((area+num)/area)^(1/2));
136 -   Elj1 = z*Eo*(((sigma/r1)^6)-((sigma/r1)^12));
137
138 -   numeric(j,1) = Xanu1;
139 -   numeric(j,3) = r1;
140 -   numeric(j,5) = Elj1;
141
142     %if num==0 %if no new sites added, E1 = -1, else use LJ
143     %E1 = Eo;
144     %else
145 -   E1 = Elj1;
```

```
146     %end
147
148     %option 2 (site added)
149 -   Xanu2 = p/(Ns+1);
150 -   r2 = vo/(((area+num+1)/area)^(1/2));
151 -   E2 = z*Eo*(((sigma/r2)^6)-((sigma/r2)^12));
152
153 -   numeric(j,2) = Xanu2;
154 -   numeric(j,4) = r2;
155 -   numeric(j,6) = E2;
156
157     %Xb calculation
158 -   eq1 = ko*Es+k1*E1*Xanu1;
159 -   eq2 = ko*Es+k1*E2*Xanu2;
160 -   xb1solve = vpasolve(log((Xanu1*(1-x)/(x*(1-Xanu1))))+(eq1-k2*Eo*x)==0,x,[10^-10 0.99999]);
161
162 -   if p> Nso*0.5 %avoid site being added early on for entropy reasons
163 -   xb2solve = vpasolve(log((Xanu2*(1-y)/(y*(1-Xanu2))))+(eq2-k2*Eo*y)==0,y,[10^-10 0.99999]);
164 -   else
165 -   xb2solve = 1000; %doesn't allow option 2 to be chosen until P > Nso*0.5
166 -   end
167
168 -   if xb1solve < xb2solve
169 -   Xanu = Xanu1;
170 -   Xbnu = xb1solve;
```

```
171 -   opt = 1;
172 -   Efinal = E1;
173 -   rfinal = r1;
174 -   else
175 -   Ns = Ns+1;
176 -   num = num+1;
177 -   Xanu = Xanu2;
178 -   Xbnu = xb2solve;
179 -   Efinal = E2;
180 -   rfinal = r2;
181 -   opt = 2;
182 -   end
183 -   Vnu = Ns - p;
184
185 -   numeric(j,7) = Xanu;
186 -   numeric(j,8) = Xbnu;
187 -   numeric(j,9) = opt;
188 -   numeric(j,10) = Ns;
189 -   numeric(j,11) = p;
190 -   numeric(j,12) = Vnu;
191 -   numeric(j,13) = num;
192 -   numeric(j,14) = Efinal; %Gamma (Lennard-Jones potential)
193 -   numeric(j,15) = Xanu*Ns/Nso; %Xa*
194 -   numeric(j,16) = Vnu/Ns; %Xv
195 -   numeric(j,17) = (Ns/area)-(Xanu*Ns/area); %V
```

```
196 -   numeric(j,18) = Xanu*Ns/area; %a
197 -   numeric(j,19) = rfinal;
198
199     %xb1solve = 0;
200     %xb2solve = 0;
201
202 -   if Xbnu > 0.99
203 -   break
204 -   end
205
206 -   end
207
208 -   toc
```

Matlab code for Checkerboard Theory

```
clc
clear
tic

%constants--------------------------------
E = -0.5; %energy for interaction between adsorbates
Es = -5.0; %energy for interaction between adsorbate and surface
sigma = 1.05 ; %ratio of sigma_aa/sigma_ss
sigmab = 1/(2^(1/6));
sig = 4*E*((sigma^6)-(sigma^12)); %L-J equation
sigb = 4*E*((sigmab^6)-(sigmab^12));
z = 5; %6*Eb*pb - 1*Eb*pb
iter = 1001; %how many iterations to run
result = [4,iter];

%calculation------------------------------
syms p1 p1i p1ii p2

for i = 1:iter
pb = ((iter-i)/(iter-1)); %bulk density

eqn1 = p1  == (p1i*p2) + ((1-p2)*p1ii);
eqn2 = p1i == pb/(pb+((1-pb)*exp(3*p2*sig + sig + Es - z*pb*sigb)));
eqn3 = p1ii== pb/(pb+((1-pb)*exp(3*p2*sig + Es - z*pb*sigb)));
eqn4 = p2  == pb/(pb+((1-pb)*exp(4*p1 + Es - z*pb*sigb)));

S = vpasolve([eqn1, eqn2, eqn3, eqn4],[p1, p1i, p1ii, p2]);

result(i,1) = pb;
result(i,2) = S.p1;
result(i,3) = S.p1i;
result(i,4) = S.p1ii;
result(i,5) = S.p2;
result(i,6) = -(3*S.p2*sig + sig + Es - z*pb*sigb);
result(i,7) = -(3*S.p2*sig + Es - z*pb*sigb);
result(i,8) = -(4*S.p1 + Es - z*pb*sigb);
end

toc
```

Curriculum Vitae

Shao-Hsuan Lin, the son of Hsi-Yung Lin and Chin-Wei Weng, was born on October 23rd, 1991 in Taipei, Taiwan. As a child full of curiosity, Shao has never hesitated to ask questions and he was relentless to find answers to the unknown. Enthralled by the thrill that overwhelms Shao whenever he unraveled a mystery; Shao realized that science is his true passion. After graduating from high school, Shao majored in chemical engineering not only because it is a promising field of study, but it is also due to his fascination with experiment processes. In order to learn more about surface phenomena, Shao decided to join laboratories that major in this area.

Shao-Hsuan Lin participated in various experiments at the Surface Phenomena Laboratory at the Department of Chemical Engineering in National Taiwan University and gained perspectives about liquid drops landing on a rough surface. After Shao got admitted by Johns Hopkins University, he was interested by the research project on adsorption compression, which describes adsorbate molecules landing on another specie's surface. Under the guidance of Professor Donohue, he completed his Master studies and met the requirements for graduation of ChemBE MSE program of Johns Hopkins University.